γ-RAYS OF NEUTRON CAPTURE

STUDIED WITH THE β-RAY SPECTROMETER

A Thesis

Submitted in Partial Fulfillment of the Requirements

for the Degree of

Doctor of Philosophy

by

Robert Edward Bell.

Faculty of Graduate Studies and Research

McGill University

April, 1948.

ACKNOWLEDGEMENTS

The author wishes to express his great appreciation to Dr. L.G. Elliott for his constant help and valuable suggestions and for much of the necessary basic technique and apparatus. Thanks are due to Dr. B.W. Sargent for his cooperation with this work in the Nuclear Physics Branch of the Chalk River Laboratory. Valuable technical assistance has been received from Miss M.L. Kolebaba and Mr. H.W.H. Walker. The operating crew of the Chalk River pile have been helpful at all times.

The author is also grateful to Dr. J.S. Foster and Dr. A.N. Shaw of McGill University for their assistance and for their kindness in allowing the present work to be done extra - murally.

Table of Contents.

ABSTRACT.

A method is described for using a β-ray spectrometer to measure the energies and intensities of the γ-rays emitted at the instant of capture of a thermal neutron by a nucleus. The method is applicable to very weak neutron capturers provided that they are available in large quantities, as well as to strong neutron capturers. Experiments were performed in which the capture γ-ray spectra of carbon, a weak capturer, and cadmium, a strong capturer, were observed.

The carbon spectrum, attributed to capture by C^{13}, contains three discrete γ-rays of approximately equal intensity having energies of 3.50 ± 0.10, 4.65 ± 0.15 and 7.15 ± 0.25 Mev. The cadmium spectrum, due to Cd^{113}, is sufficiently complex so that individual γ-rays were not resolved. The hardest γ-rays detected in the capture γ-ray spectrum of Cd^{113} had an energy of 6.2 ± 0.15 Mev, These results for the γ-rays of neutron capture were shown to be consistent with theoretical expectation.

In preliminary experiments, new results were obtained on the disintegration scheme of Cs^{134} (1.7 year) and on an upper limit for the intensity of a 3.20 Mev γ-ray of ThC".

CHAPTER I. INTRODUCTION

I. Statement of the Problem.

The purpose of this study is to make an examination of the γ-rays emitted at the instant of neutron capture by various nuclear species. For this purpose, use is being made for the first time of a β-ray spectrometer to study the electrons ejected by the γ-rays from secondary radiators. This method of studying γ-rays enables the line structure of a γ-ray spectrum to be measured with a resolution of the order of 5% or better. The object of this report is to introduce the method and to present experimental results for the γ-rays of neutron capture of carbon and cadmium.

The importance of the study of γ-rays of neutron capture lies in the fact that the capture of a thermal neutron in a nucleus of mass number A gives to the compound nucleus A+1 an excitation energy of several Mev, equal to the binding energy of the neutron in the ground state of the nucleus A+1. The final nucleus A+1 loses its energy of excitation by the emission of one or more γ-ray quanta. A measurement of the total energy radiated in the form of γ-rays then gives the binding energy of the neutron, which in turn gives the mass difference between the capturing nucleus A and the final nucleus A+1 (See Section III below). In addition, and perhaps more important, the nucleus A+1, raised to a high excitation level by the neutron capture process, may lose its energy by the emission of several γ-rays in succession. The study of the energies and intensities of these γ-rays yields information about the energy levels of the nucleus concerned. The study of such nuclear energy levels is of great importance because it is one of the main keys to an understanding of the structure of the nucleus.

II. Discovery.

The discovery that γ-rays are usually emitted at the instant of capture of a neutron by a nucleus was made by Fermi and his collaborators in 1934 (1) in the course of their pioneer work on neutron-induced radioactivity. Fermi's experiments showed that most cases of neutron activation were due to "simple capture" reactions of the type (n,γ), and he correctly proposed that neutron absorption which did not result in radioactivity of the absorber was usually due to a similar capture process with the formation of a stable isotope. He was able to detect the γ-radiation accompanying neutron capture in both cases. Among the lighter elements, there are four known cases where neutron capture is followed by particle emission, and, as Fermi showed, little or no γ-radiation then accompanies the capture process. Above Z = 8, simple capture accompanied by γ-radiation is the predominant process. For most capturing elements, Fermi showed that the capture cross-section is very much greater for thermal neutrons than for those of higher energies. Since the time of Fermi's work, the capture γ-rays have been qualitatively observed many times, but only a few experiments, necessarily rather inaccurate, have been directed towards measuring the quantitative character of this γ-radiation. A summary of these attempts is given later (Section V).

III Binding Energy of the Neutron.

The study of the γ-rays of neutron capture yields the most direct measure of the mass difference between the capturing nucleus and the final nucleus. Since the total excitation energy of the final nucleus is equal to the binding energy of the neutron in this nucleus, the measured total energy emitted as γ-radiation, E_o (Mev), gives the mass difference directly:

$$\Delta M = M_n - \frac{E_o}{931}, \qquad (1)$$

where ΔM is the mass difference, M_n is the mass of the neutron, and 931 is the energy equivalent in Mev of one atomic mass unit.

It follows from these statements that a prediction of the total energy emitted as γ-radiation in any particular neutron capture reaction depends on a knowledge of the mass difference between the capturing nucleus and the final nucleus. Among the light elements (up to about Z = 20) many of these differences are known from mass-spectrographic studies or from the energy balances of nuclear reactions, and the estimation of the binding energy is straightforward. For heavier elements, theoretical mass formulas must be employed.

A formula for the mass of any nucleus (A,Z) has been given by Weizsacker (2) and Bethe (3). The formula is semi-empirical in character, based on the statistical liquid-drop model of the nucleus, with the coefficients of the various terms adjusted to fit experiment. We take the formula in the form given by Fermi (4):

$$M(A,Z) = 0.99389\,A - 0.00081\,Z + 0.014\,A^{2/3} + 0.083\,\frac{(A/2-Z)^2}{A} + 0.000627\,\frac{Z^2}{A^{1/3}} + \delta\,,$$

where $\delta = 0.036\,A^{-3/4}$ (A even, Z odd) (2)

$\delta = -0.036\,A^{-3/4}$ (A even, Z even),

$\delta = 0$ (A odd).

In the neutron capture reaction, A is increased by unity and Z is unchanged, so that the mass difference due to neutron capture is

$$\Delta M(A,Z) = M(A+1,Z) - M(A,Z).$$

Hence $\Delta M = \frac{\partial}{\partial A}\left[M(A,Z)\right]$ with an error < 0.001 mass units for A = 20 and negligible above A = 40,

so that
$$\Delta M = 1.01464 + 0.0093\, A^{-1/3} - 0.083\,\frac{Z^2}{A^2} - 0.000209\, Z^2 A^{-4/3} + \Delta\delta, \qquad (3)$$

where

$\Delta\delta = 0.036\, A^{-3/4}$ for A even, Z even or A odd, Z odd: i.e. for N even, where N=A-Z = number of neutrons,

$\Delta\delta = -0.036\, A^{-3/4}$ for A even, Z odd or A odd, Z even: i.e. for N odd.

The binding energy in Mev then becomes

$$B.E. = 931\left[M_n - \Delta M\right]$$
$$= 77.3\, Z^2 A^{-2} + 0.195\, Z^2 A^{-4/3} - 8.66 A^{-1/3} - 5.30 + \Delta E,$$

where

$$\Delta E = 33.5\, A^{-3/4} \quad (N \text{ odd}) \qquad (4)$$
$$= -33.5\, A^{-3/4} \quad (N \text{ even})$$

In every case, A and Z refer to the capturing nucleus. It is seen that, according to this result, all nuclei are divided into two classes so far as the binding energy of the captured neutron is concerned: capturing nuclei having odd N yield a systematically higher binding energy than those having even N. Of the naturally occurring stable isotopes, the great majority (including all the most abundant isotopes) have even N.

On account of the discontinuous and non-unique way in which A varies with Z throughout the periodic table, it is of course not possible to plot a smooth curve of the neutron binding energy as a function of Z for the natural elements. A sort of average plot can be made, assuming A to vary with Z according to the Weizsacker - Bethe maximum nuclear stability formula, again using the form given by Fermi (4):

$$Z_A = \frac{A}{1.981 + 0.015A^{2/3}} \qquad (5)$$

The result is a pair of curves of binding energy versus Z, the upper one for odd N and the lower one for even N, as plotted in Fig. 1. The curves can only give the general trend of binding energy, and values for individual isotopes will in general not lie on the curves, but will cluster around them in the same way as the natural isotopes cluster around the maximum stability curve (ref. 3, Fig. 2.). In addition, the curves fail rather badly at low Z, as expected from a statistical formula. This is illustrated in Fig. 1 by the points representing the binding energy of the captured neutron in light isotopes, calculated from the experimental masses in Mattauch's table (5).

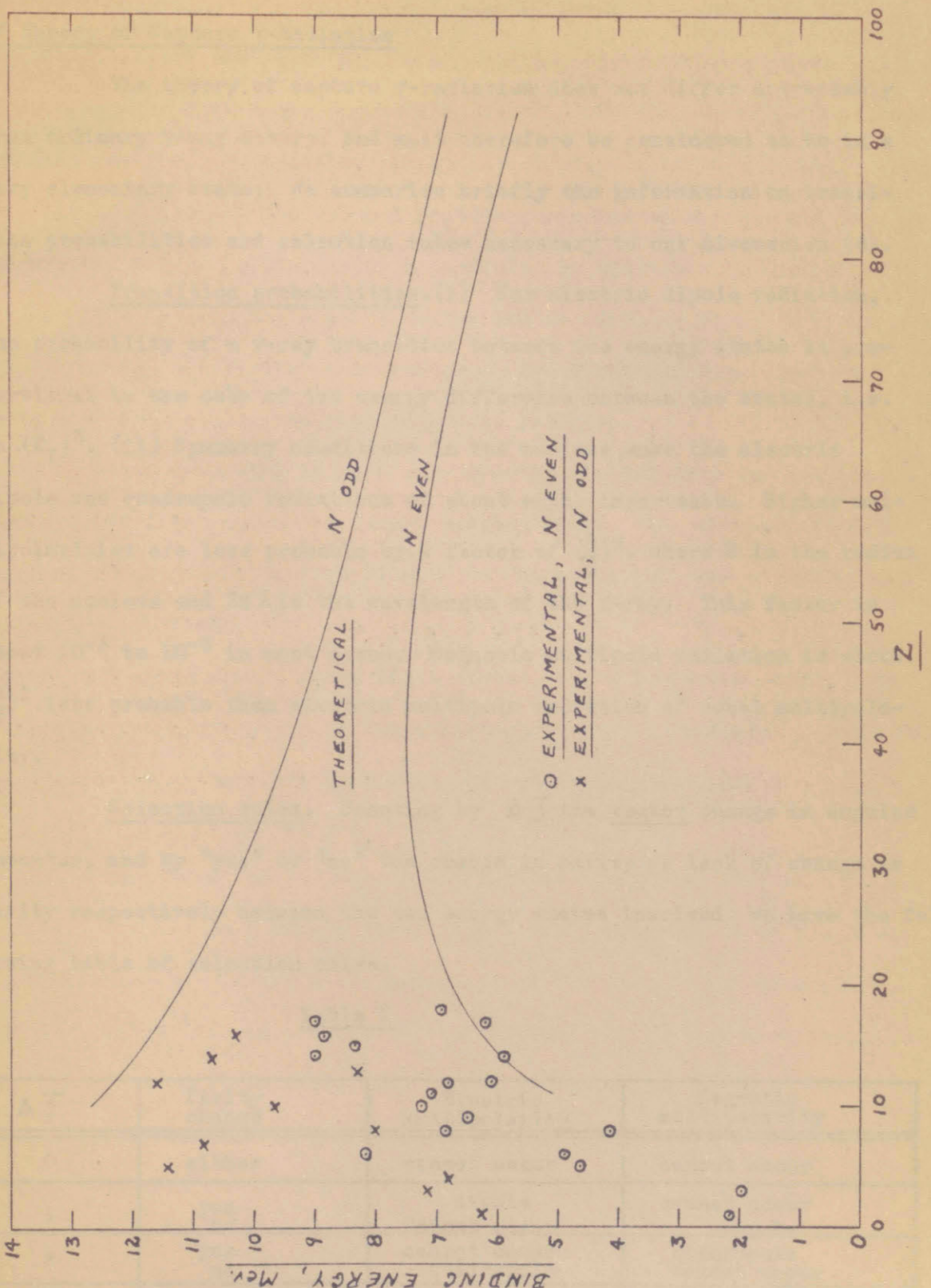
BINDING ENERGY, Mev.
Z
THEORETICAL
N ODD
N EVEN
○ EXPERIMENTAL, N EVEN
× EXPERIMENTAL, N ODD

Figure 1

IV Theory of Capture γ-Radiation

The theory of capture γ-radiation does not differ appreciably from ordinary γ-ray theory, and must therefore be considered to be in a very elementary state. We summarize briefly the information on transition probabilities and selection rules necessary to our discussion (6).

Transition probabilities. (i) For electric dipole radiation, the probability of a γ-ray transition between two energy states is proportional to the cube of the energy difference between the states, i.e. to $(E_\gamma)^3$. (ii) Symmetry conditions in the nucleus make the electric dipole and quadrupole radiations of about equal importance. Higher multipolarities are less probable by a factor of $(\frac{R}{\lambda\!\!\!^{-}})^2$, where R is the radius of the nucleus and $2\pi\lambda\!\!\!^{-}$ is the wavelength of the γ-ray. This factor is about 10^{-3} to 10^{-4} in most cases. Magnetic multipole radiation is about $(\frac{R}{\lambda\!\!\!^{-}})^2$ less probable than electric multipole radiation of equal multipolarity.

Selection rules. Denoting by $\Delta \vec{j}$ the vector change in angular momentum, and by "yes" or "no" the change in parity or lack of change in parity respectively between the two energy states involved, we have the following table of selection rules.

Table I

$\Delta \vec{j}$	Parity change	Electric multipolarity	Magnetic multipolarity
0	either	cannot occur	cannot occur
1	yes no	dipole cannot occur	cannot occur dipole
2	yes no	cannot occur quadrupole	quadrupole cannot occur
3	yes no	2^3-pole cannot occur	cannot occur 2^3-pole

According to a distinction made by Bethe (7), only the first γ-ray emitted after the capture of a neutron is a true capture γ-ray: all succeeding ones come under the heading of ordinary γ-rays from the excited residual nucleus. The distinction is not of much experimental use, because, while it is true that the primary capture γ-ray has an energy depending on the kinetic energy of the captured particle, in dealing with the capture of thermal neutrons, the kinetic energy can be taken as zero. The theoretical consideration of the γ-ray spectrum which accompanies neutron capture does, however, require the distinction to be made.

The discussion is most conveniently divided into two sections, dealing with light and heavy nuclei respectively. This division is arbitrary, and the transition from "light" to "heavy" is of course gradual and not clearly defined.

Light nuclei. Among light nuclei, thermal neutron capture may produce a reaction leading to the emission of charged particles because of the low potential barriers involved. An outstanding example is

$$_5B^{10} + {}_0n^1 \rightarrow {}_3Li^7 + {}_2He^4 + 2.9 \text{ Mev}$$

Of the excess energy of 2.9 Mev, about 2.5 Mev appears as kinetic energy and about 0.4 Mev as a single γ-ray (8,9). This reaction is of practical importance because it has a cross-section of 700 barns * for natural B (20% B^{10}, 80% B^{11}). This cross-section follows the 1/v law accurately (10) and, since the reaction gives rise to soft γ-radiation, boron is useful as a shielding and calibrating material. An (n,α) process also occurs on Li^6, with a cross-section of 70 b for the mixed isotopes of Li, and no γ-radiation (7).

---

* 1 barn = 10^{-24} cm.^{2}, abbreviated to b.

Reactions of the simple capture type (n,γ) also occur among light nuclei, and our interest centers on these. Because of the large spacings of the energy levels in light nuclei (order of Mev, as indicated by proton capture experiments), it seems very likely that the entire binding energy of the neutron would in many cases be emitted as a single primary γ-ray. The direct transition is most probable if it is electric dipole or quadrupole, because the transition probability increases rapidly with energy, and the wide spacing of the levels means that alternative transitions have much lower energy. The measurement of this γ-ray energy then would give the mass difference between the capturing and final nuclei by equation (1). A hypothetical scheme illustrating this situation is given for C^{12} in Figure 2. Since C^{12} has angular momentum j = 0 (20), the excited C^{13} (denoted C^{13*}) can only have j = 1/2, since a thermal neutron can only carry in an angular momentum equal to its own spin of 1/2. Since C^{13} has j = 1/2 (20), the direct γ-ray transition to the ground state is dipole radiation (See Table I), and should be more probable than any other mode of de-excitation of C^{13*}. The total energy available is 4.90 Mev, from Mattauch's mass table (5). The situation for capture by C^{13} is somewhat more complicated, and will be used to illustrate a case where the direct transition to the ground state may not occur. Starting from j = 1/2 for C^{13}, the compound C^{14*} could have j = 0 or 1. The angular momentum of the ground state of C^{14} is known to be zero (47). The two possible situations in this case are illustrated in Fig. 3 (a) and (b) for the angular momentum of C^{14*} = 1 and 0 respectively. In (a), the direct transition is electric dipole radiation, and therefore should occur more than any other. In (b), the direct

transition cannot occur, and an indirect path, such as that suggested in the diagram, must be followed. In capture by C^{13}, the total energy available is 8.16 Mev.

Heavy Nuclei. The spacing of energy levels in heavy nuclei is perhaps 0.2 Mev near the ground state, judging by nuclear γ-rays in the natural radioelements. This spacing decreases rapidly with increasing energy of excitation (about as $k_1 e^{-k_2 \sqrt{E}}$, where E is the excitation energy (7)), so that there are a relatively large number of energy levels on which γ-ray transitions from the excited state formed by the neutron capture could end. It is therefore to be expected on the present theoretical view that the primary γ-ray would not carry away all the available energy in every case, even where it is allowed. We thus expect a rather complicated γ-ray spectrum resulting from neutron capture in heavy elements, and the observation of a single primary γ-ray carrying all the neutron binding energy is much less probable. Bethe (7) has calculated a theoretical energy spectrum for the allowed primary γ-rays of neutron capture in heavy elements for an energy level spacing of 10 volts at the full excitation energy. His result is given in Fig. 4. In the diagram, $I_{E\gamma}$ is the relative intensity of γ-rays of energy E_γ, and E_o is the total excitation energy, equal to the neutron binding energy. The figure applies only to the primary capture γ-rays, and is not meant to suggest that a continuous γ-ray spectrum is present, but only that a very complex spectrum is to be expected. The choice of different energy level spacings does not alter the result much unless very large spacings are chosen, i.e. the light element case. It is seen from Fig. 4 that according to Bethe's result, comparatively few γ-rays are emitted with the full excitation energy, E_O, or anything

approaching it. With this picture, it is possible to obtain the binding energy from measurements on the capture γ-rays only if a complete de-excitation scheme for one mode of successive γ-ray emission is obtained.

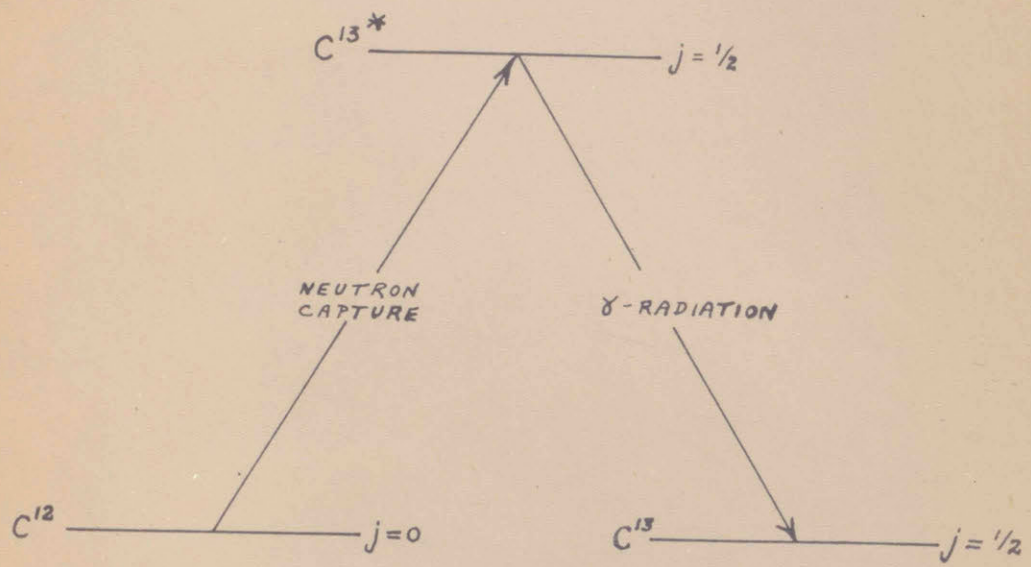

Figure 2

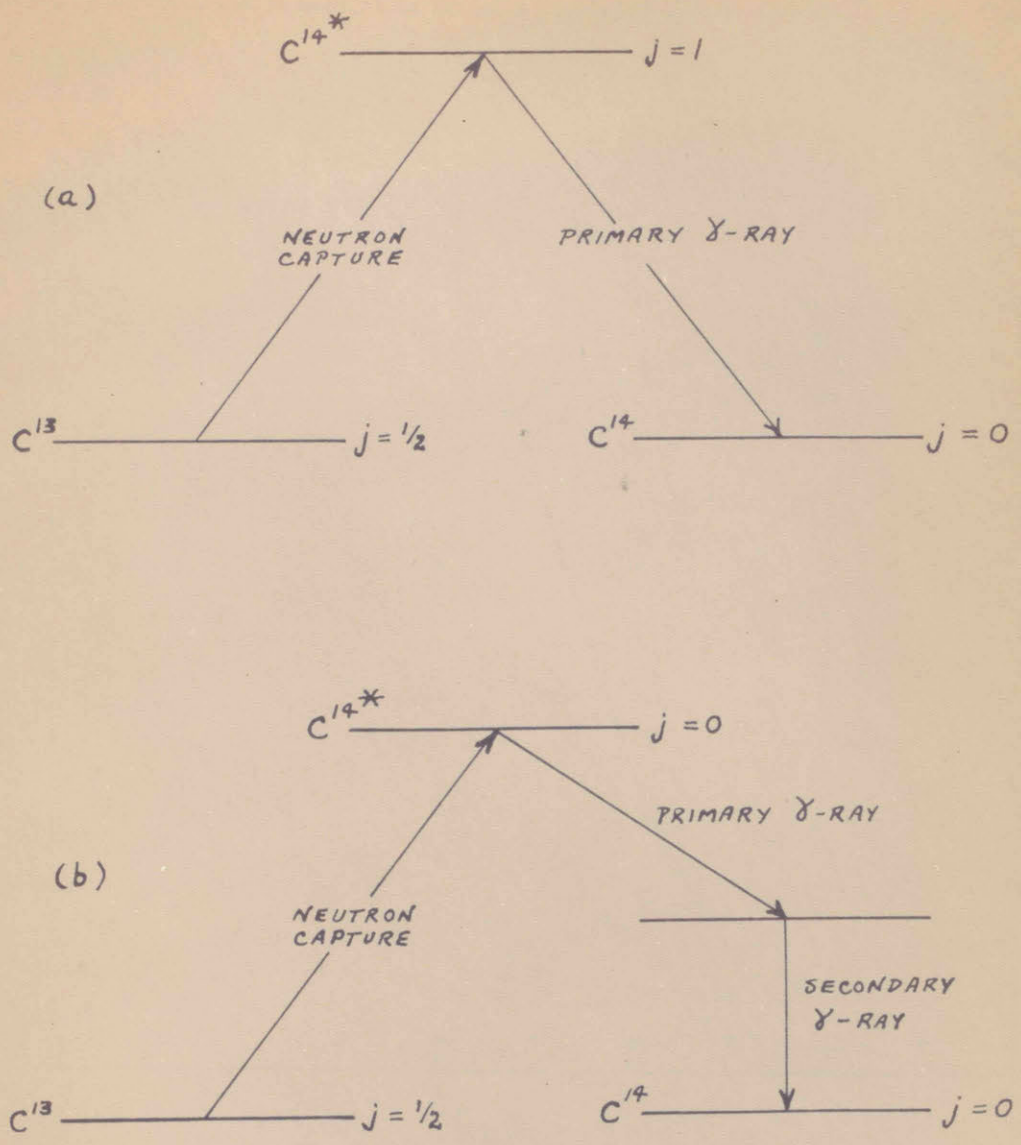
(a)
C^{14*}
j = 1
NEUTRON CAPTURE
PRIMARY γ-RAY
C^{13}
j = ½
C^{14}
j = 0
(b)
C^{14*}
j = 0
PRIMARY γ-RAY
NEUTRON CAPTURE
SECONDARY γ-RAY
C^{13}
j = ½
C^{14}
j = 0

Figure 3

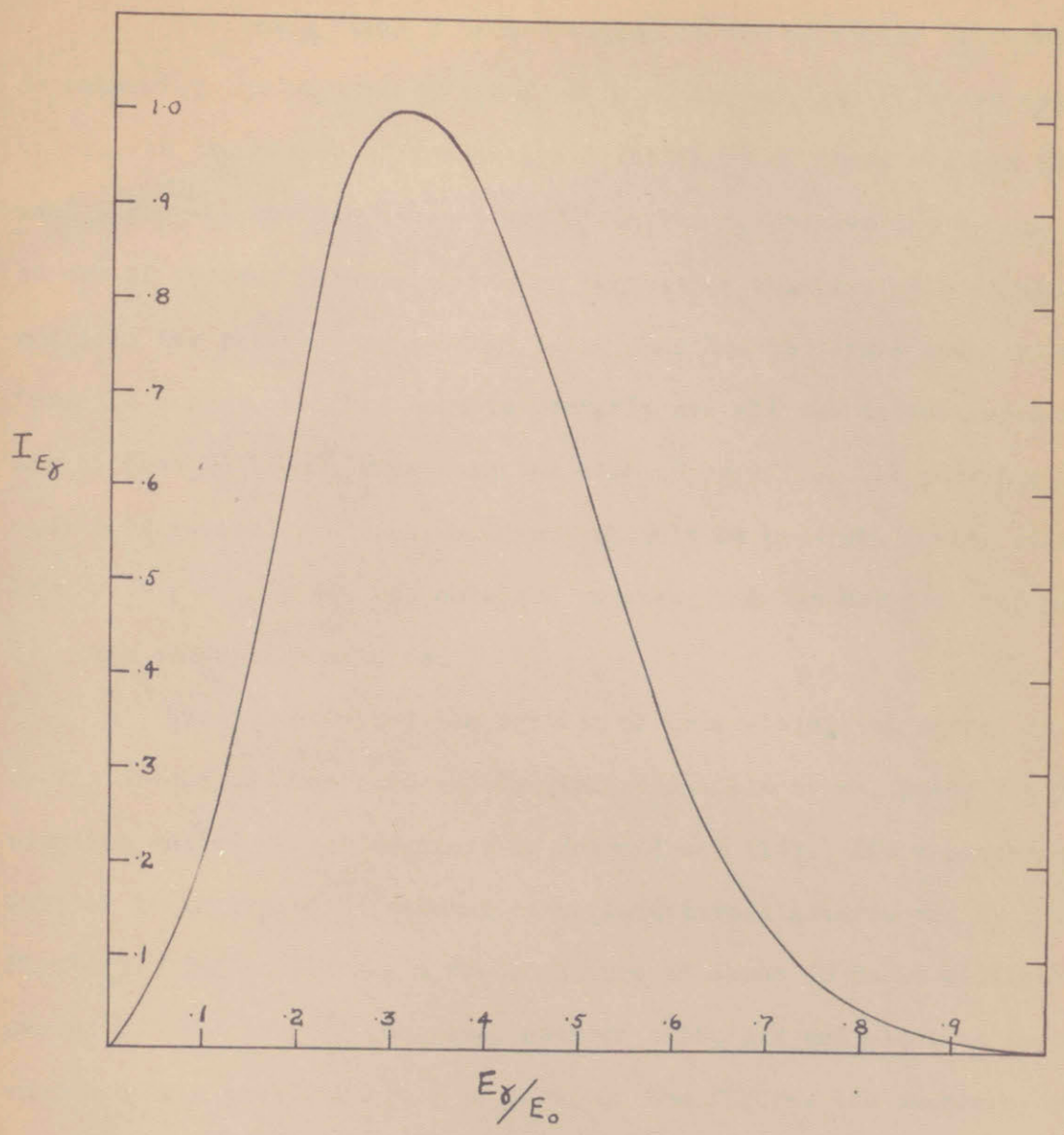

Figure 4

V. Previous Work on Capture γ-Rays.

Following Fermi's demonstration of the existence of γ-radiation accompanying the capture of neutrons, a number of investigators attempted to examine the nature of the γ-rays. The first of these was Lea (11). He used a Ra-α-Be neutron source, and attempted to observe the γ-rays scattered out of various materials with an ionization chamber. His effects were small in the presence of a large background due to γ-rays and fast neutrons from the source, and his results probably are all due to inelastic scattering of fast neutrons, except in the case of paraffin. In paraffin, a large number of thermal neutrons would undoubtedly be present, giving rise to γ-rays by capture in H. Lea obtained an energy of 3-4 Mev for this radiation by rough absorption methods.

Rasetti attacked the problem of determining the energy of the γ-rays by the method of absorption of Compton recoil electrons, using two thin aluminum-walled Geiger counters in coincidence (13). His arrangement is similar to that used by several subsequent investigators, and is shown in Figure 5. The source was a Po-Be mixture of about 60 to 90 millicuries strength. The source, counters, neutron capturers and electron absorbers were enclosed in a paraffin block as shown in the figure, the counters being shielded from the source by a cone of lead. After being slowed down to thermal energies in the paraffin, the neutrons are captured in one of the blocks of capturing material A, B. Some of the resulting capture γ-rays generate Compton recoil electrons in the nearest wall of a Geiger counter C,D; such electrons will give rise to coincidences when both counters are traversed. The absorption of the coincidences by means of Al or Pb plates E placed between the counters gives a measure of the γ-ray energy. Rasetti

judged the energies of the γ-rays from the half and quarter - thicknesses of Al or Pb, assuming as a calibration that the γ-rays from the source were of 5 Mev energy. The mixed energies of the γ-rays meant that Rasetti's half and quarter-values did not agree with each other, the amount of the disagreement presumably furnishing an indication of the inhomogeneity. Rasetti gave figures for Cl, Co, Y, Ag, Cd, Ir and Hg. His results are collected in Table III (below), cols. 4 and 5, at the end of this section.

Fleischmann (14) used a Radon-α-Be source of neutrons enclosed in a large lead block in his work on neutron capture γ-rays. The γ-rays from the source were thus attenuated, and the nature of the γ-rays generated by the capture of neutrons in a large plate of the capturing material was studied by means of absorption in lead in front of a Geiger counter. RaC and ThC γ-rays were used as a calibration of the absorption apparatus. He obtained 1.5 Mev for the γ-ray of capture of a neutron in H by this method. He also observed the γ-rays from Cu, Fe, Cd and Pb. The results are collected in Table III, col. 6.

In a later series of measurements, Fleischmann (15) attempted to determine the absolute yield of γ-quanta per neutron captured in various elements. His neutron source was the same as in the previous work, and he used a carbon-walled Geiger counter to detect the γ-rays. On the basis of his previous measurements on the energies of the γ-rays, and some assumptions as to the efficiency of the Geiger counter as a function of energy, he arrived at the results given in Table II. Here the first column gives the capturer, the second Fleischmann's "relative number of quanta per neutron absorbed", and the third gives the number on the basis of H (paraffin) = 1. The validity of the results seems open to question.

Table II.

Capturer	Relative No. of Quanta	Absolute No. of Quanta
Cd	1.13	1.21
Cu	0.87	0.94
Fe	0.80	0.86
Paraffin	0.93	1.00
Pb	1.71	1.84
Ag	1.06	1.14

In a still later work, Fleischmann (16) turned to the Compton - coincidence method, the arrangement being identical with that of Rasetti except for the neutron source. His γ-ray energies were estimated from the half-thickness value of the Compton electron absorption curve in Al. He examined H, Al, Fe, Cu, Se, Ag, Cd, Sm, Gd, Hg and Pb. The results are given in Table III, col.7.

Haenny (17) used absorption in lead to estimate the quantum energies of the capture γ-rays from Cl, Gd, Cd, Hg and Au. His results are rather rough, and appear in Table III, col.8.

Kikuchi, Husimi and Aoki in a long series of papers, (18), have investigated the γ-rays emitted from many elements under bombardment by both fast and thermal neutrons. Only the thermal neutron results will be quoted. These investigators obtained their neutrons from the D on D reaction (19), bombarding D_2O ice with deuterons at 300 kv from a high voltage rectifier set. The yield of neutrons was equivalent to a Ra-α-Be source of several curies and was nearly free of γ-rays. Their main method of determining the energy of the capture γ-rays was again the Compton - coincidence absorption method,

but in this case reliance was placed chiefly on the end-point of absorption curve in Al. The absorption end-point gives only the γ-ray of highest energy present in appreciable intensity, but some estimates of possible lower energy components were made by noting the shape of the absorption curve. On this basis, the γ-rays from Cl, Cu, Fe, and Cd were thought to be inhomogeneous. RdTh and Ra (B+C) γ-rays were used for calibration of the absorption curves. The results of these investigators, consisting of a large number of careful measurements throughout the periodic table, are given in Table III, col. 3.

Table III summarizes the main experimental evidence on the energy of the γ-rays liberated at neutron capture by a large number of elements from H to Pb. The headings of the columns are self-explanatory, except for Col. 9, which contains the total binding energy of the neutron in the elements shown. Figures in brackets are calculated by formula (4): other figures are calculated from Mattauch's table of masses. The binding energy is given for the isotope mainly responsible for capture (20) or, where this is not known, for the most abundant isotope.

The results of Table III seem to show that the most energetic γ-ray of appreciable intensity (which is what is detected by the Compton - coincidence end-point) from many neutron capturers has an energy of the order of 0.8 or 0.9 of the total excitation energy due to the capture of the neutron, while from others the maximum is as low as 0.55. This fact is not expected from the theory of Bethe, represented by Figure 4, where the highest energy γ-ray of appreciable intensity is at perhaps 0.6 of the maximum, and large changes in this figure from element to element are not predicted. We are thus led to think that at least in some cases the capture γ-ray spectra may contain more high - energy γ-rays than predicted

by the Bethe theory. The main conclusion from Table III is, however, that the composition of the γ-ray spectrum due to neutron capture is unknown for all elements, and that on this account little or no information about the total neutron binding energy can be obtained from the experimental data.

One or two other experimental studies on capture γ-rays may be mentioned. Pontecorvo (21) has studied the γ-rays from Au bombarded with slow neutrons whose energy composition was varied by means of boron absorbers. The γ-ray energy was estimated by absorption in lead, and Pontecorvo believed that the spectral composition of the Au γ-rays varied with the energy composition of the neutrons. In view of the experimental difficulties involved, this result must be treated with reservation. Burhop, Hill and Townsend (22) measured the absorption in boron of the neutrons which excited γ-rays in Cd, Ag, Sb, I and Hg. In the case of the latter three, the absorption curves consisted of superimposed fast and slow varying components, due to capture resonances at different energies. The conclusion presumably is that all neutrons captured, whether of resonance energy or not, produce γ-rays.

Aoki (23) has attempted to find the average number of γ-rays emitted in each capture process, for Cd, Ni and Hg. The method involved two counters in coincidence, with rather arbitrary assumptions about the γ-ray efficiencies of the counters. The results given are:

Cd - about 3 γ-rays per neutron.

Ni and Hg - about 2 γ-rays per neutron.

The chief value of this experiment is to show that coincidences do occur, so that in at least some fraction of the cases, more than one γ-ray emerges

per neutron captured. The result for Cd is in marked disagreement with the result of Fleischmann for Cd (Table II).

Table III.

1	2	3	4	5	6	7	8	9
Element	Z	Husimi et al. max. γ energy	Rasetti 1/2 thickness	Rasetti 1/4 thickness	Fleischmann Ref. 14	Fleischmann Ref. 15	Haenny	Total γ energy
H	1	2.13 ± 0.15			1.5	2.26		2.18
Al	13	4.05 ± 0.29				5.8		8.25
Cl	17	6.15 ± 0.24	6.6				6	9.0
K	19	5.0 ± 0.49						(9.05)
Ti	22	5.0 ± 0.73						6.9
Cr	24	6.85 ± 0.48						(7.16)
Mn	25	5.45 ± 0.36						(6.14)
Fe	26	6.6 ± 0.24				7.7		(7.93)
Co	27	6.6 ± 0.36	5.0	5.0				(7.87)
Cu	29	6.15 ± 0.36			2.5	7.4		(8.16)
Zn	30	5.7 ± 0.49						(8.95)
As	33	5.1 ± 0.36						(7.10)
Se	34	5.7 ± 0.36				5.8		(6.16)
Br	35	5.1 ± 0.24						(7.44)
Y	39	4.75 ± 0.49	4.0	4.1				(7.29)
Ag	47	4.4 ± 0.37	3.6	4.1		3.7		(7.07)
Cd	48	5.1 ± 0.24	4.1-4.5	4.5-5.3	2.1	4.1	10	(8.55)
Sb	51	4.05 ± 0.37						(6.61)
I	53	4.75 ± 0.49						(6.52)
Sm	62	4.75 ± 0.37				3.3		(8.13)
Gd	64					4.0	7-8	(7.93)
W	74	4.75 ± 0.37						(5.79)
Ir	77		3.3	4.4				(5.95)
Au	79	5.2 ± 0.48						(6.06)
Hg	80	5.9 ± 0.72	5.3	5.0		4.5	15	(5.81)
Pb	82				0.45	4.2		(5.99)

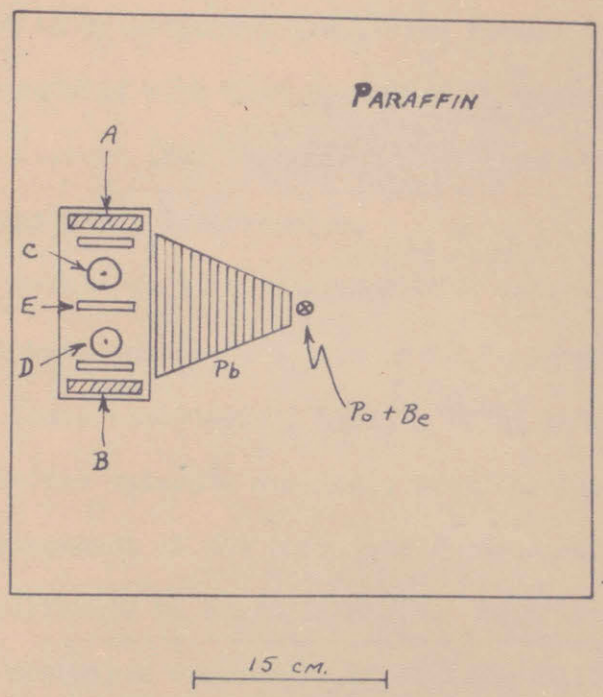

Figure 5

CHAPTER 2. METHOD AND APPARATUS

I. Method of γ-ray Spectrometry

The capture γ-rays are studied by using a β-ray spectrometer to analyse the secondary electrons ejected by the γ-rays from various radiators. The method was first applied by Ellis and Aston (24) in the case of the 180° focusing β-ray spectrometer, and by Skobeltzyn (25) in cloud-chamber studies. A review of such methods has been published by Latyschev (26). The method followed here agrees in many details with that described by Deutsch, Elliott and Evans (27) and Elliott (28) for artifically radioactive substances, using a thin lens β-ray spectrometer.

The method will be described with reference to some preliminary experiments done on a source of Rd Th in equilibrium with its products. These experiments, besides being intrinsically interesting, yielded valuable auxiliary data for the main experiments. The arrangement of the thin lens β-ray spectrometer for the preliminary experiments is shown in Fig.6. This type of spectrometer has been described very fully by Deutsch, Elliott and Evans (27). Electrons in a definite momentum interval are focused on the counter by the magnetic field of the coil. Different momentum intervals are selected by varying the current in the coil, and since no iron is used in the system, the momentum is proportional to the current. The width of the momentum interval selected is directly proportional to the momentum of the electrons focused. The source arrangement is shown in Fig.7. The radio-active source is surrounded by sufficient material of low atomic number (Aℓ) to stop all the primary β-rays. The secondary

electrons ejected from the Al cap (Fig.7) are then almost entirely Compton recoil electrons, since the photoelectric and pair production cross-sections are small at low Z. The experimental counting rate from this source, plotted as a function of the momentum of the recoil electrons, is shown as a broken curve in Fig.8. The recoil electron spectrum, for a γ-ray of given energy E_γ extends from zero up to a definite maximum energy given by

$$E_{max} = E_\gamma \frac{2E_\gamma}{2E_\gamma + mc^2} .$$

Such distributions as that of Fig.8 can be used to determine the energy of a single γ-ray, but the resolution of close γ-rays is difficult. The addition of a thin radiator of an element of high atomic number, as shown in Fig.7, gives rise to monoenergetic groups of photoelectrons as well as the recoil electron distribution (solid curve, Fig.8). Taking account of the fact that the photoelectric conversion can take place in the K,L ... shells of the atoms of the radiator, the difference between the two curves is practically a line spectrum of the γ-ray source. The energy of each electron group must have added to it the K.L ... binding energy of the radiator atoms, to give the γ-ray energy.

In order to obtain the greatest line intensity, the high atomic number radiator should be made as thick as possible up to the point where an appreciable fraction of the emerging electrons no longer fall within the momentum interval selected. In addition, the atomic number of the radiator should be made as high as possible, since the photoelectric cross-section increases about as the 4.5 power of Z(29).

The influence of these factors for the case of the 2.62 Mev γ-ray of ThC" - ThD is shown in Figure 9. In particular, this figure shows an increase of about 60% in line height for a nearly constant radiator thickness, due to the change in radiator material from Pb (Z = 82) to U (Z = 92). It also shows that at this energy, no significant increase in line height can be obtained by increasing the radiator thickness above about 150 Mg/cm^2. The permissible radiator thickness increases about linearly with energy but since the photoelectric cross-section varies about as 1/E in the high-energy region (30), it should be possible to maintain the photoelectron line height shown in Fig.9 up to very high γ-ray energies.

An additional aid to unravelling a complex γ-ray spectrum is the observation of the positrons ejected from the high-Z radiator by the pair-production process. The positrons may be separated from the electrons in the spectrometer by means of a spiral-finned baffle, as described in Ref.27. With such a baffle in the spectrometer, the positrons or electrons may be observed at will by merely reversing the current in the coil. A typical pair of curves, due to the 2.62 Mev γ-ray of ThC" - ThD, is shown in Fig. 10. The positron spectrum is a continuum ending sharply at (2.62 - 2 mc^2) Mev = 1.60 Mev, and having a shape agreeing well with that calculated by Jaeger and Hulme (31). For higher γ-ray energies, the positron end-point becomes less abrupt, and the spectrum of the positrons and electrons from pair-production becomes identical.

In Fig.10, which was taken with the spectrometer in its final experimental arrangement, the line-width of the photoelectron

line is about 3% at half-height, or 6% at the base. Due to this finite line-width, both the Compton electron continuum and the positron continuum extend about one line-width beyond their respective theoretical end-points.

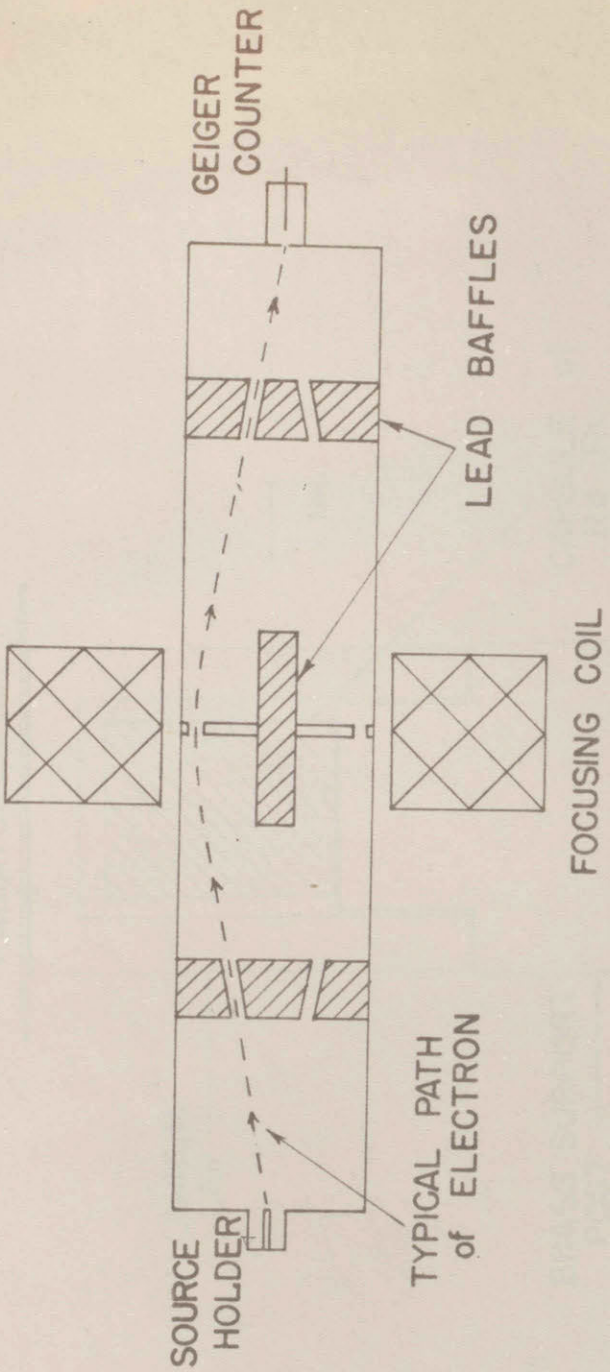
GEIGER COUNTER
LEAD BAFFLES
FOCUSING COIL
TYPICAL PATH of ELECTRON
SOURCE HOLDER

Figure 6

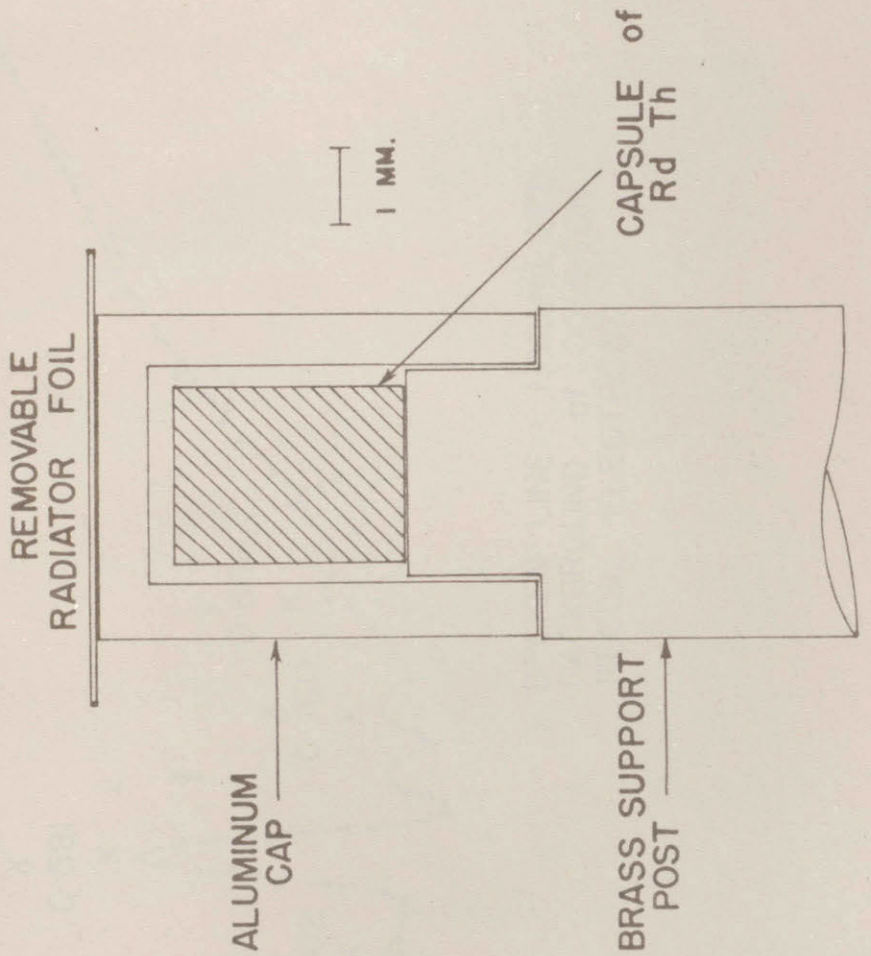
REMOVABLE
RADIATOR FOIL
1 MM.
CAPSULE of
Rd Th
ALUMINUM
CAP
BRASS SUPPORT
POST

Figure 7

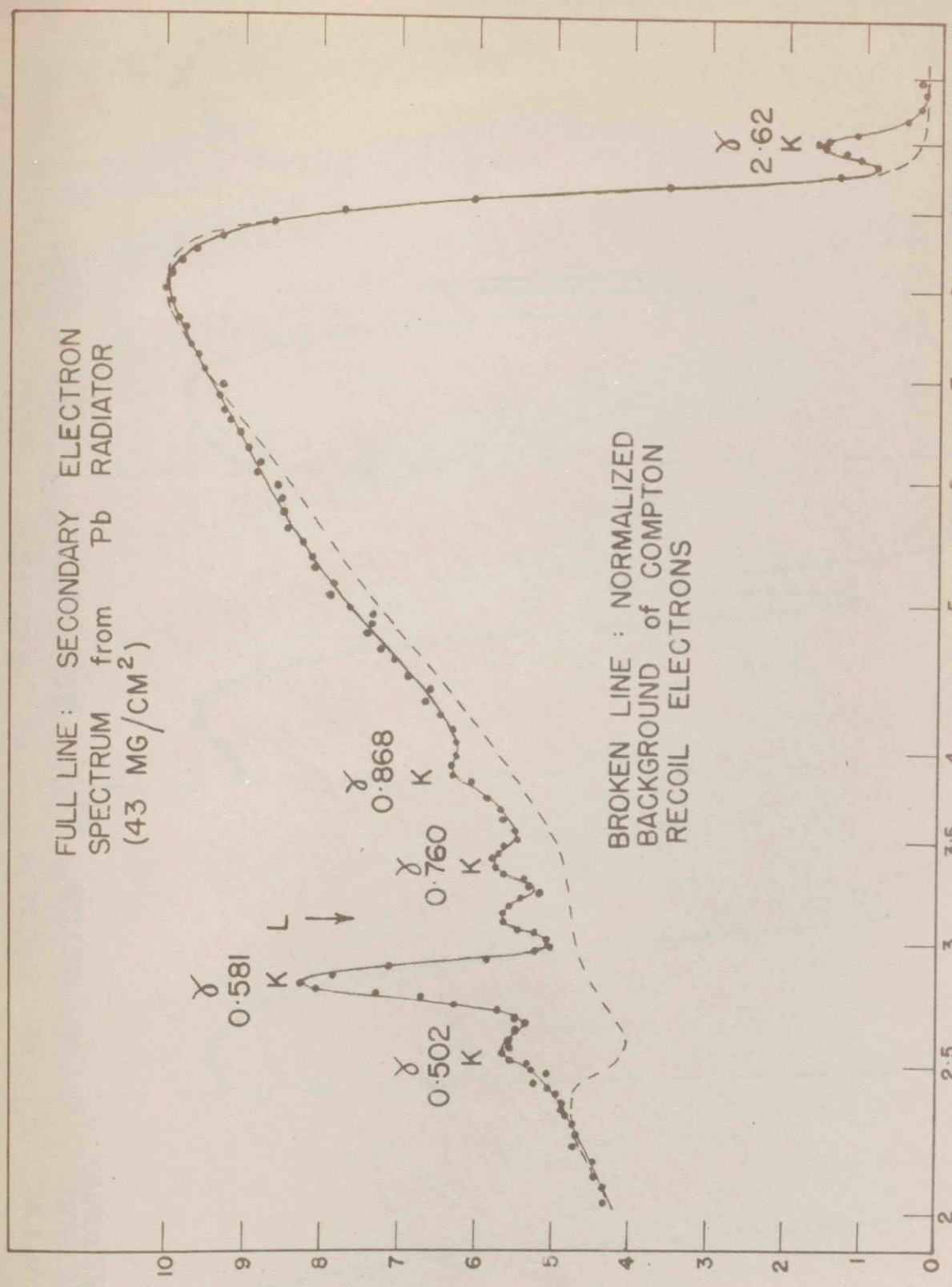
FULL LINE : SECONDARY ELECTRON SPECTRUM from Pb RADIATOR (43 MG/CM²)
BROKEN LINE : NORMALIZED BACKGROUND of COMPTON RECOIL ELECTRONS
γ 0·581 K L
γ 0·502 K
γ 0·760 K
γ 0·868 K
γ 2·62 K
RELATIVE COUNTING RATE
Hρ (10³ GAUSS – CM.)
0
1
2
3
4
5
6
7
8
9
10
11
2
2·5
3
3·5
4
5
6
7
8
9
10
11

Figure 8

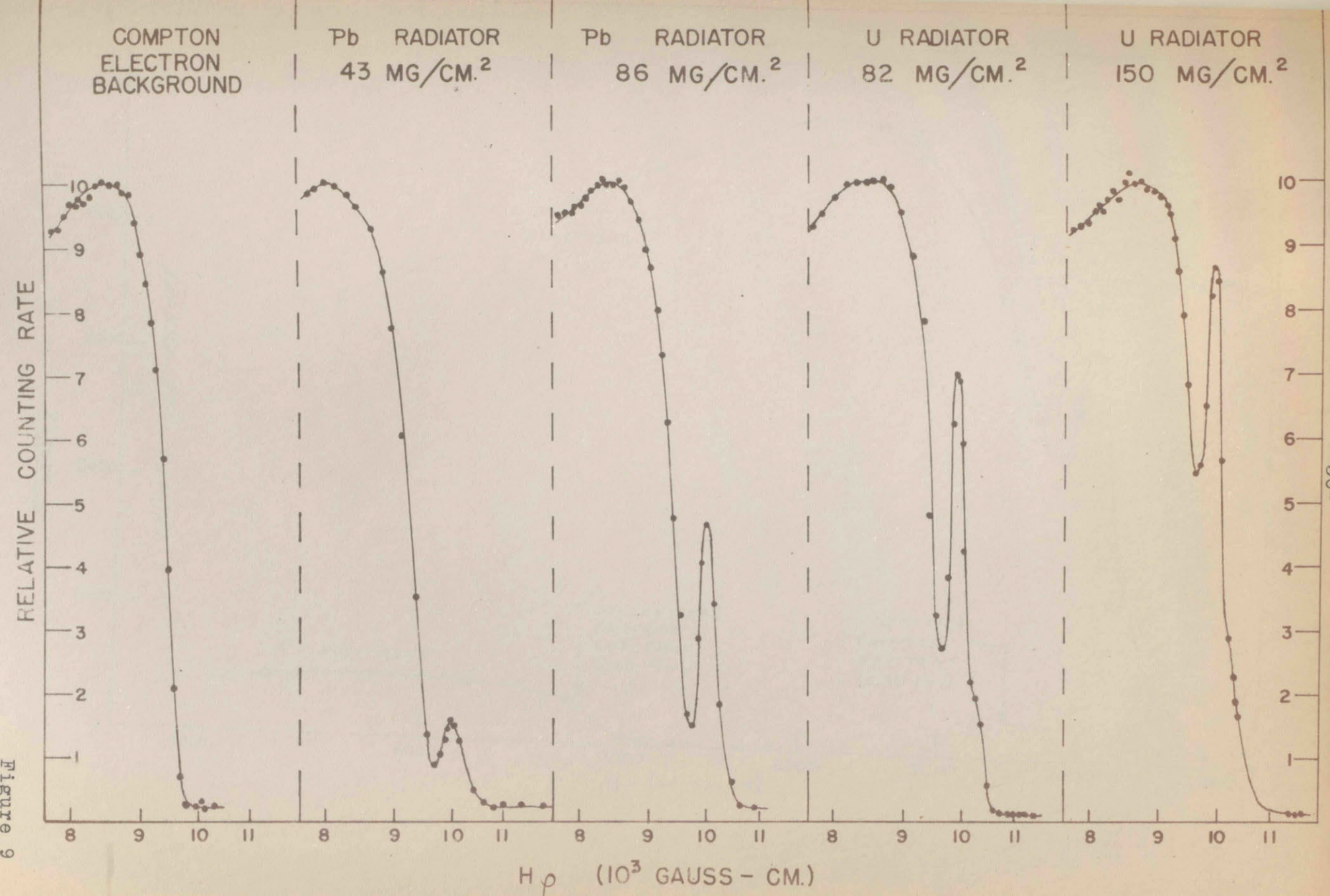
COMPTON ELECTRON BACKGROUND
Pb RADIATOR 43 MG/CM.²
Pb RADIATOR 86 MG/CM.²
U RADIATOR 82 MG/CM.²
U RADIATOR 150 MG/CM.²
RELATIVE COUNTING RATE
Hρ (10³ GAUSS - CM.)

Figure 9

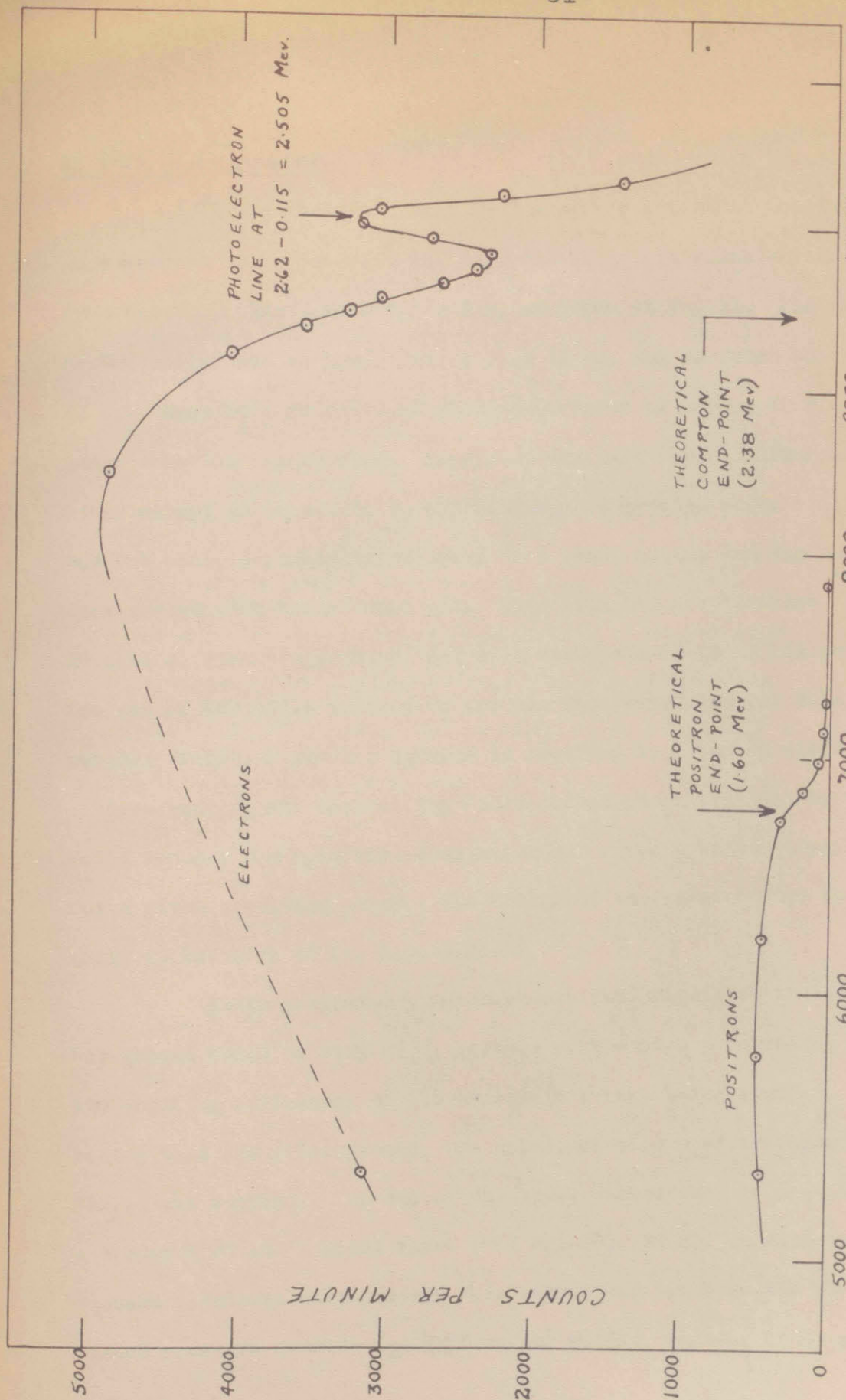
PHOTOELECTRON
LINE AT
2·62 - 0·115 = 2·505 Mev.
ELECTRONS
POSITRONS
THEORETICAL
POSITRON
END-POINT
(1·60 Mev)
THEORETICAL
COMPTON
END-POINT
(2·38 Mev)
COUNTS PER MINUTE
Hρ (GAUSS-CM)
0
1000
2000
3000
4000
5000
5000
6000
7000
8000
9000
10,000
11,000

Figure 10

II β-Ray Spectrometer.

The spectrometer used in the main experiments consisted of an evacuated brass tube 100 cm. long and 20 cm. in diameter, and two symmetrically placed focusing coils, as shown in Fig.11. The windings of the coils have an inner diameter of 22 cm. and an outer diameter of 62 cm. Each coil consists of about 3600 turns of number 10 B & S gauge enameled copper wire. Layers of 1/4 inch copper tubing are interspersed at intervals in the windings to provide water cooling, and the whole assembly is enclosed in a brass casing and vacuum impregnated with transformer oil. Each coil has a resistance of about 15 ohms at room temperature, and will dissipate about 12 kilowatts. The use of two coils instead of one has two advantages for this application: first, a smaller current is required to focus an electron of a given energy, and second, the field distribution provided by two coils reduces the spherical aberration and gives a better transmission for a given resolving power. The design of the spectrometer tube and coils is the work of Dr. L.G. Elliott.

Rough preliminary measurements indicated that the counting background would be very high, because of the high penetrating power and counting efficiency of the energetic γ-rays being studied. To reduce this γ-ray background, the coincidence counter arrangement of Fig.11 was adopted. The end of the spectrometer tube is provided with a window W of .001" dural sheet ($\sim$7 mg/cm^2), 18 mm. in diameter. The focused electrons pass through this window and traverse the thin-walled aluminum counter C_1 ($\sim$30 mg/cm^2 walls), causing it to pulse as

they pass through. The actual focus of the spectrometer is at the 8 mm. hole in the 3 mm. thick brass diaphragm D, and electrons which pass through this hole register in the mica-window β-ray counter C_2. True focused electrons then cause coincident pulses in C_1 and C_2. The efficiency of this arrangement in reducing background may be judged from the fact that, in a particular case, 1400 coincidences due to focused electrons were observed per minute against a background of 600 coincidences per minute, while the γ-ray background in C_1 alone was 10,000 counts per minute. The coincidence arrangement thus reduces the background by a factor of 16.

An incidental but very important benefit of the coincidence counting arrangement is that it almost eliminates the dependence of the counting rate on the counting characteristics of the individual counters. The slope of the plateau in an ordinary Geiger counter is mainly caused by two factors (1) the enlargement of the sensitive volume as the voltage is raised (2) the occurrence of spurious pulses following a true count. The geometrical arrangement of the coincidence counters eliminates (1) and the coincidence arrangement eliminates (2) except for the entirely negligible number of chance coincidences. The two counters together constitute a detector of unusual stability, and very reproducible results have been obtained with them.

The arrangement has the disadvantage that it is sensitive only to electrons of energy high enough to penetrate the window W and the walls of C_1 without too much scattering. Experiments with C_1 replaced by a temporary counter with very thin walls showed that this effect is negligible at 5 Mev, but that it reduces the counting rate to one-half at 2.5 Mev.

The source end of the spectrometer was provided with a bismuth cylinder bored with a conical hole tapering at a half-angle of 15° down to 6 mm. diameter at the inside of the spectrometer. The Bi cylinder fitted into a hole counter-bored into the lead door of the thermal column of the Chalk River pile, and the conical hole was continued through the 10 inch thickness of the lead door. The conical hole in the lead door and in the Bi cylinder could be fitted with neutron-absorbing linings (Cd, B_4C) for neutron collimation, or left unlined for γ-ray collimation, when the neutrons are stopped inside the door. The end of the Bi cylinder at the spectrometer was closed by .020" copper sheet for the vacuum seal.

Inside the spectrometer, (see Fig.11), a lead cone tapering from 4" diameter to 1/2" diameter in a length of 10 inches absorbed most of the γ-rays leaving the source in the direction of the counter. The space marked "baffle" is filled either with an ordinary annular baffle (See Fig.6) or a spiral positron-electron baffle (see Ref.27), usually the latter.

As indicated in Fig.10, the spectrometer in this arrangement has a line width of the order of 3% at half height. The solid angle through which transmission is obtained is of the order of 0.1% of the sphere. The energy calibration is taken from Fig.10, assuming the photoelectron peak to consist of electrons of energy 2.505 Mev from the 2.620 Mev γ-ray of ThC" - ThD.

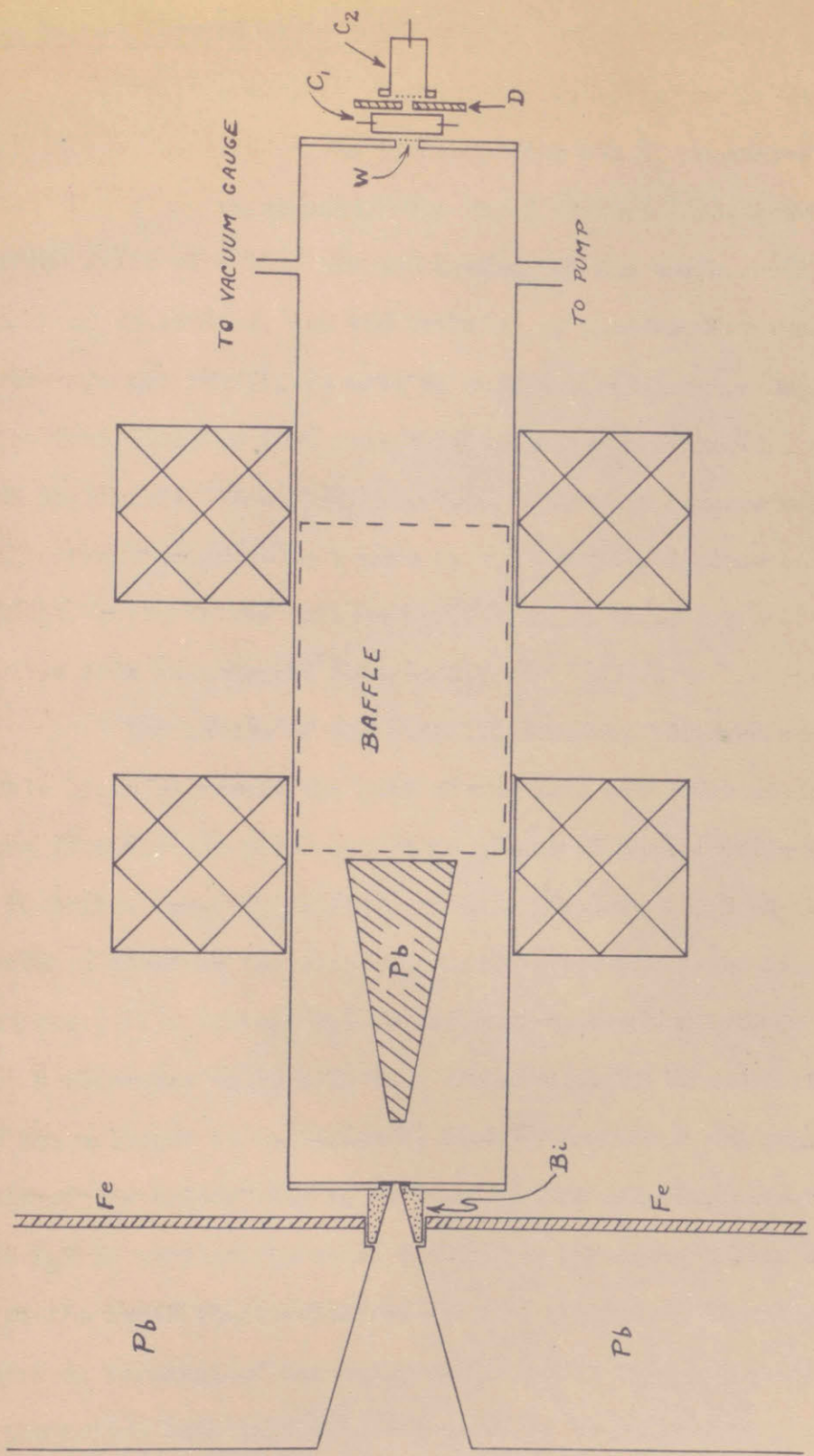

Figure 11

III. Magnet Current Stabilizer.

The accuracy of relative energy measurements with the β-ray spectrometer depends on the accuracy with which the current in the coils is set and maintained. The chief factors tending to make the current drift with time are the heating of the coils, with consequent change of resistance, and the drifting of the output voltage of motor-generators and rectifiers used to supply the current. Rapid changes in current, such as that caused by generator brush noise, must also be made negligible. The stabilizer built for this purpose maintains the coil current constant to 1 part in 10^4 and is self-balancing in its action: currents are changed by altering a small d-c reference voltage derived from an accurate potentiometer.

The action of the stabilizer can be followed on Fig.12. The double lines represent the path of the main coil current. The current flows from the d-c power source to ground through a large bank of 36 or 72 triode tubes (type 6AS7) in parallel. From ground it flows through a standard resistance R_S and through the coil, back to the generator. The voltage $R_S I$ across the standard resistance is compared with a reference voltage V_R in a d-c amplifier. The difference between the two voltages is amplified by the d-c amplifier and impressed on the grids of the triode bank so as to alter the current in such a direction that $R_S I$ is very nearly equal to V_R. At the same time an a-c amplifier takes the rapid fluctuations of voltage ("ripple") from the high-potential terminal of the coil, amplifies it and applies it to the grid of the triode bank in such a direction as to cancel the ripple voltage of the coil.

Both d-c and a-c amplifiers apply their signals to the grids of the main triode bank through a mixer amplifier.

The degree of equality of $R_S I$ and V_R, or the degree of cancellation of the ripple voltage, is easily shown to be greater, the greater the gain around the feedback loop concerned. The following amplifier gains have been provided:

d-c amplifier (0 to 10 cycles) - 60,000

a-c amplifier (10 to 500 cycles) - 100

mixer amplifier (0 to 500 cycles) - 5

main triode bank (0 to 500 cycles) 1

Since, in a typical set of conditions, the standard resistance may be 1/9 ohm and the coil resistance 15 ohms, we have

$$\text{gain around d-c loop} = 60{,}000 \times 5 \times \frac{1}{9} \times \frac{1}{15} = 2{,}200$$

$$\text{gain around a-c loop} = 100 \times 5 = 500.$$

It is easily shown that a drift or fluctuation is reduced by the stabilizer to $\frac{1}{G+1}$ of its value, where G is the loop gain. Thus the stabilizer reduces any tendency to drift by $\frac{1}{2200}$, so that an original drift of 22% is held within 1 part in 10^4. The point in having the d-c gain so high is not the anticipation of d-c drifts of the order of 22%, but the fact that the stabilizer is expected to change currents in the coil by moderate factors following a simple change in the reference voltage V_R. Under the conditions stated, the stabilizer should be able to start from conditions of perfect balance and change the current by 22% in either direction without adjustment other than the change in V_R, still holding the current accurate to 1 in 10^4. This performance is in fact realized, and enables the automatic switching of coil currents with high accuracy (see Section IV below).

The order of magnitude of the reference voltage V_R is 1 volt, so that when $V_R = R_s I$ to 1 part in 10^4, the d-c error signal impressed on the d-c amplifier input is about 10^{-4} volt. Conventional electronic d-c amplifiers are incapable of amplifying signals of so low an amplitude without drift, but a d-c amplifier of special design (Fig.13) has been built to accomplish this end. In Fig.13, the two potentials V_R and $R_s I$ are applied to terminals A and B. These d-c voltages pass through resistance - capacity filters, designed to eliminate hum and spurious pickup, to the terminals 1 and 2 of a Brown converter (32). This device is a double-throw switch operated at 60 cycles by an auxiliary winding. The output at terminal 3 of the converter thus consists of a square wave of 60 cycle frequency, and peak-to-peak amplitude $|V_R - IR_s|$. This square wave is amplified in a conventional 60-cycle amplifier (gain = 240,000) emerging at the secondary of transformer T_1 as a wave of average amplitude $120{,}000\ |V_R - IR_s|$. The phase-sensitive detector in Fig.13 consists of a pair of diodes synchronously opened and closed by transformer T_2. The resulting filtered d-c output of the phase-sensitive detector is $60{,}000\ |V_R - IR_s|$, and the d-c output voltage changes sign as $V_R - IR_s$ changes sign. The whole assembly thus acts as a true d-c amplifier of gain 60,000, stable and free of drift.

The a-c amplifier is a single conventional resistance - capacity coupled stage (type 6SJ7), as shown in Fig.14. This diagram also shows the mixer amplifier (6V6), and the method of adding the outputs of the d-c and a-c amplifiers at the grid of the mixer.

The main triode bank, not shown in a diagram, consists merely of 36 or 72 tubes (type 6AS7 twin-triode) connected in parallel, with a 2000 - ohm stopping resistor in each grid lead. The heaters are supplied in groups of 18 tubes in series from the 110 volt line. A single bank of 36 tubes will pass 10 amperes plate current with a voltage drop of 50 volts across the tubes, a performance not equalled by any other known tube or comparable combination of tubes.

The reference voltage V_R is supplied by a logarithmic potentiometer* supplied by a storage battery and calibrated against a standard cell, using the stabilizer itself as a null indicator. The logarithmic potentiometer gives 60 steps of voltage, each step increasing the voltage by 2%. The range covered is from 0.5 volt to 1.63 volts. An interpolation knob enables any intermediate voltage to be selected. The logarithmic scale provided by the potentiometer is a convenience in examining electron distributions, because the spectrometer has a constant fractional line-width $\frac{\Delta(H\rho)}{H\rho}$ (See Section I), so that, when plotted on a logarithmic scale of current or $H\rho$, all lines have the same width. Changing the coil current by 2% merely requires changing the logarithmic potentiometer switch by one step: the current then automatically adjusts itself to the new value within 1 part in 10^4 within a few seconds.

The standard resistances* are made of Cenco resistance wire, which has zero temperature coefficient at room temperature, in values of 3, 1, 1/3, 1/9 and 1/18 ohm. selected by a switch. The relative values of the resistances are correct to 1 part in 10^4.

*Designed by Dr. L.G. Elliott.

The d-c power supplies consisted of three motor generators and a rectifier type power supply, as listed here:

TABLE IV

Type	Max. Volts	Max. Amps.	Max K.W.
Motor-generator	250	50	12.5
Motor-generator	270	45	7.5
Motor-generator	300	20	5
Rectifier set	350	50	18

These units could be connected in any series combination. The generator voltages could be varied by means of the shunt field rheostats, from about 20% of maximum voltage upwards, but the output voltage of the rectifier set was fixed at the value shown.

The stabilizer as described above will handle currents from 0.167 amperes to about 15 amperes without modification. For higher currents, and for increased safety, the following steps were taken:

(1) a resistance of 10 ohms was placed in parallel with the main triode bank, so that the stabilizer controlled only a portion of the current. When two coils are used in series (30 ohms), this step ensures that no more than 1/4 of the applied voltage (up to 800 volts) can appear across the triode bank.

(2) the control voltage on the grids of the main triode bank was used to control a smaller triode bank in series with the shunt field of one of the generators, thus increasing its output voltage at higher

currents. This step in effect increases the loop gain of the d-c system by adding a second d-c loop: the result is a 50% wider range of current variation for a given setting of the controls, when the current is being varied by V_R alone.

(3) while running at high power, the coils were protected from burning out in case of a water supply failure by connecting up a Wheatstone bridge in which two arms were the coil resistance and the standard resistance, and the third and fourth arms were auxiliary wire-wound resistors. The bridge supply voltage was the d-c voltage across the coil, and any unbalance of the bridge could only be due to a heating of the coil with consequent resistance change. The unbalance was indicated by a Weston Sensitrol relay, and a change in resistance of 30% in the coils (temperature rise = 100°C) would cause the relay to close and throw off the generators.

The current system contains a large number of meters, switches, fuses and circuit breakers not described more fully because they exist merely for convenience and safety. The entire instrument, apart from the generators and coils, is housed on a single standard relay rack.

In designing the stabilizer to be free of oscillation and hunting (i.e. low-frequency oscillation), the books of Bode (33) and McColl (34) were referred to. In the design, the Nyquist criterion (35) for feedback amplifier stability was used as a guide. This criterion may be stated as follows: Suppose the total gain of the feedback loops to be plotted versus frequency; if, at all points of the curve where the gain exceeds unity, the magnitude of the slope of

of the curve is less than 6 db per octave, the stabilizer will be stable and overdamped; if between 6 db and 12 db per octave, it will be stable and underdamped; if over 12 db per octave, it will be unstable. The chief practical rule derived from this criterion is that the frequency response of any amplifier plus feedback loop should be limited, if possible, by a single RC time constant (which gives 6 db per octave), and that the cascading of nearly identical RC time constants will cause oscillation. No great difficulty was experienced in making the device stable, as soon as these conditions were satisfied.

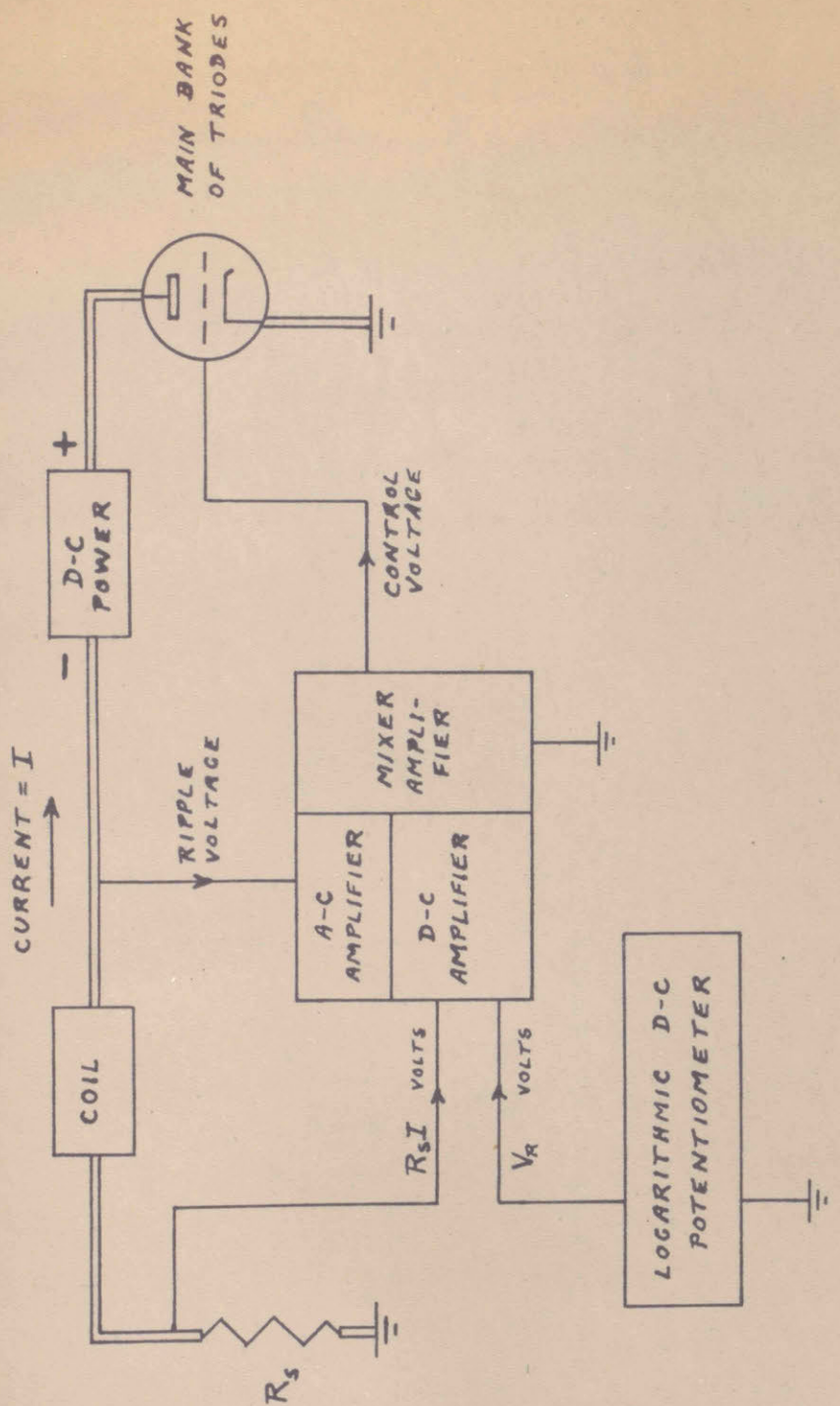
MAIN BANK OF TRIODES
+
D-C POWER
−
CONTROL VOLTAGE
MIXER AMPLI-FIER
CURRENT = I
RIPPLE VOLTAGE
A-C AMPLIFIER
D-C AMPLIFIER
COIL
R_sI VOLTS
V_R VOLTS
LOGARITHMIC D-C POTENTIOMETER
R_s

Figure 12

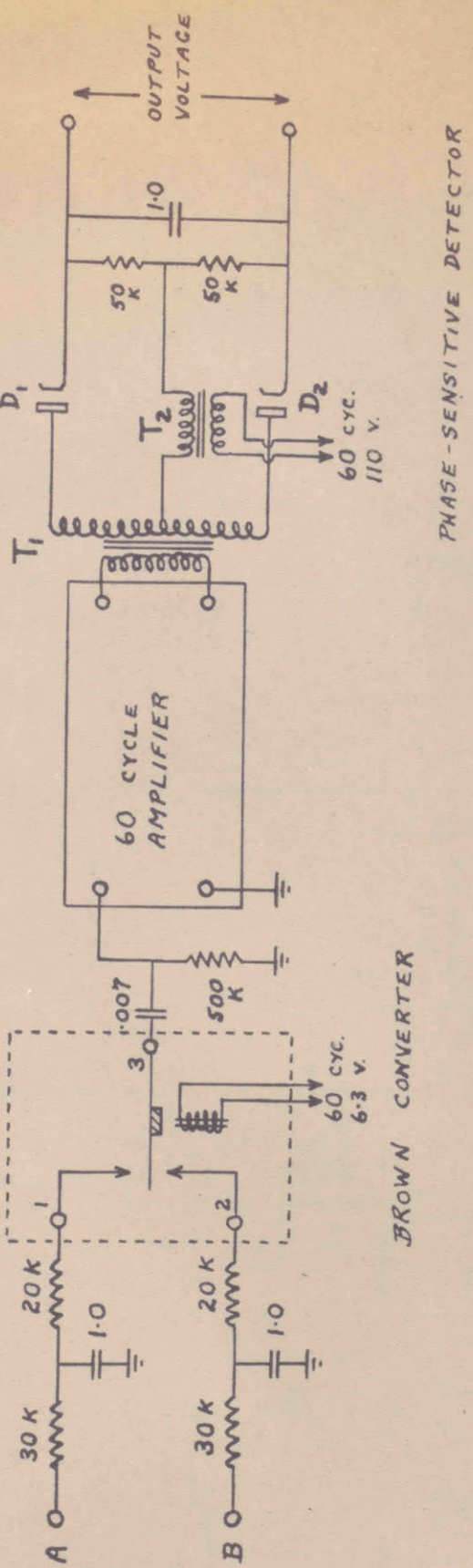
OUTPUT VOLTAGE
1.0
50 K
50 K
D1
T2
D2
60 CYC. 110 V.
T1
60 CYCLE AMPLIFIER
.007
500 K
3
60 CYC. 6.3 V.
1
2
20 K
20 K
1.0
1.0
30 K
30 K
A
B
PHASE-SENSITIVE DETECTOR
BROWN CONVERTER

Figure 13

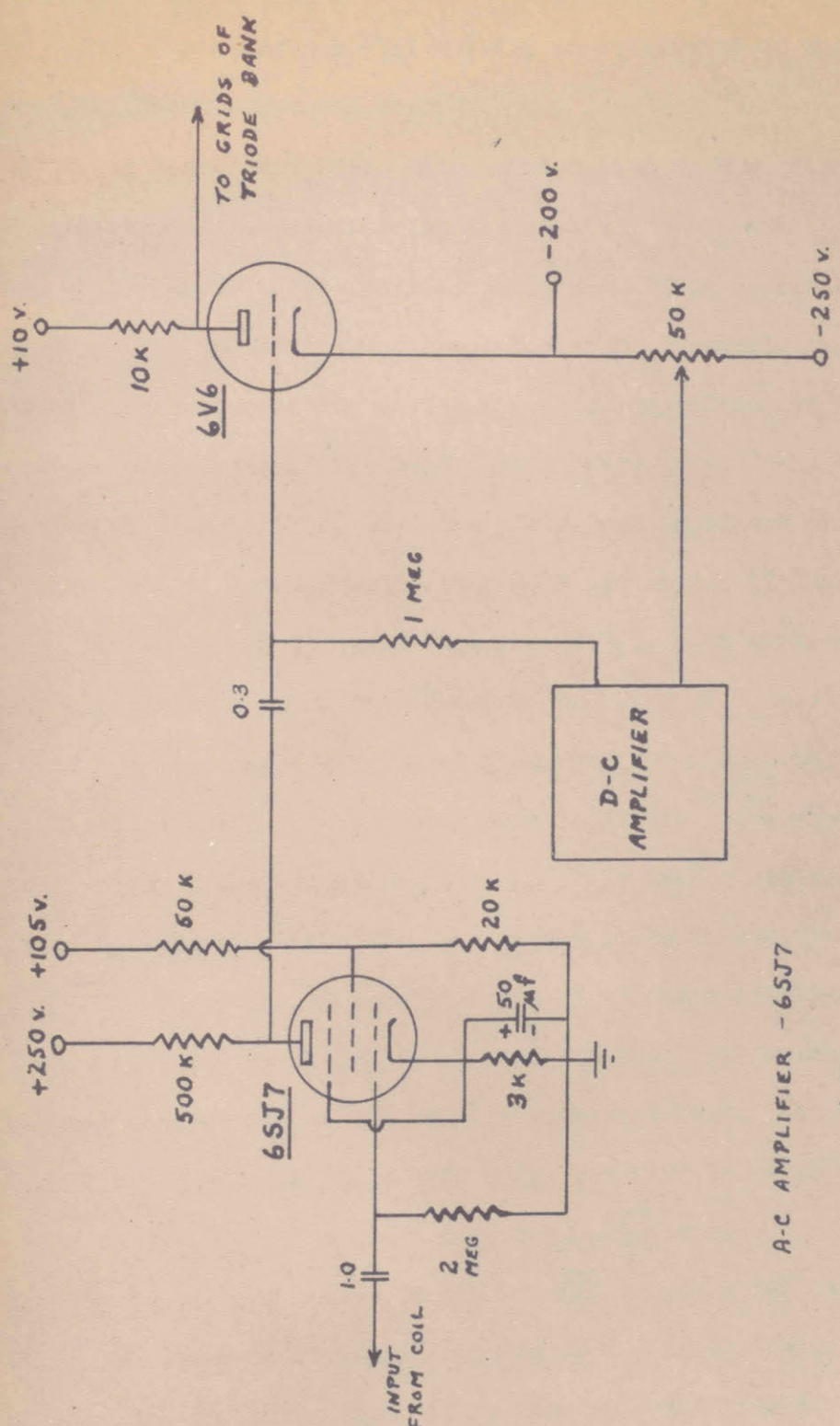
+10 V.
10K
6V6
TO GRIDS OF TRIODE BANK
-200 V.
50 K
-250 V.
1 MEG
0.3
D-C AMPLIFIER
+105 V.
60 K
20 K
+250 V.
500 K
6SJ7
+150 MF
3K
2 MEG
1.0
INPUT FROM COIL
A-C AMPLIFIER - 6SJ7
MIXER - 6V6

Figure 14

IV. Auxiliary Apparatus.

This section will briefly describe some of the instruments used in the experimental arrangement.

(1) Coincidence amplifier. The requirements on the coincidence amplifier used for registering the counts from C_1 and C_2 (Fig.11) are mainly those of reliability and freedom from spurious electrical pickup. The amplifier used consisted of two channels (one for each counter, each consisting of two stages of amplification) and a coincidence mixer stage. The design of a single one of the amplifying stages is shown in Fig. 15. The plate load impedance of the pentode V_1 consists of L and C with diode D in parallel. (C includes the plate capacity of V_1 and the grid capacity of V_2). The application of a sharp negative - going wave front to the grid of V_1 would, except for the diode D_1 cause a ringing of frequency $f = \frac{1}{2\pi\sqrt{LC}}$ in the plate circuit, as shown by the dotted line in Fig.15. The diode cuts off the ringing after one half cycle, giving a half - sinusoidal plate pulse of length $\pi\sqrt{LC}$. The gain of the stage is easily shown to be $g_m\sqrt{L/C}$. The stage will not respond at all to positive-going wave-fronts because the diode D then cuts off the first half-cycle. Slowly-varying wave-fronts of either sign have no effect. In the present amplifier, L = 0.100 mh, C = 20 uuf, V_1 = 6AC7 ($g_m = 10^{-2}$), and we have

$$\text{gain of stage} = g_m\sqrt{L/C} = 22$$

$$\text{pulse length} = \pi\sqrt{LC} = 0.13 \times 10^{-6} \text{ sec.}$$

The coincidence mixer stage consists of a similar circuit with two tubes in parallel replacing V_1. Coincident pulses at the two grids cause a

pulse of double size at the plate, and suitable circuits select only the double size pulses for counting. The coincidence resolving time is varied by varying L and C, and thus is stable and independent of tube characteristics. The resolving time has been varied by this means between 0.08 and 1.75 x 10^{-6} sec. with good results. The latter figure was used for all the main experiments, and the amplifier proved very reliable.

(2) Neutron flux monitor. In order to monitor the effective neutron flux for the experiment, (the flux varied due to changes in pile operating conditions and changes in the experimental arrangement) a Geiger γ-ray counter was placed near the source end of the spectrometer. Enough γ-rays were observed in this region (due to neutron capture in the collimating holes, etc.) to operate the counter at rates of 2000 to 10,000 counts per minute. This counting rate was continuously recorded on the moving tape of a graphic ammeter by means of a counting rate meter. The latter meter is of a special design incorporating scaling circuits for range changing and a built-in 60 cycle calibration circuit, and is considered accurate to 1%. The resulting record of effective neutron flux was used together with records from a pile operating ionization chamber, to correct the observed counting rates in the spectrometer.

(3) Counter Voltage supply. All the counters used in this experiment were supplied with highly stable voltage by a single stabilized voltage supply. The circuit of this voltage set is almost identical with that of the magnet current stabilizer. The d-c generators are replaced

by a 2000 V. 15 ma. power supply, the main triode bank by a single high voltage triode type HK-25G, and the mixer amplifier tube by a second HK-24G. The reference voltage is supplied by a standard cell, and the comparison voltage is obtained from a voltage divider of wire-wound resistors. The output voltage of the device is 1500 volts ± 0.01%, with current capacity 15 ma. Each counter is supplied with variable voltage by means of an accurate voltage divider made of wire-wound resistors, enabling the individual counter voltages to be varied continuously from 500 to 1500 volts independently of one another. The power supply has run continuously for over one year with only minor replacements.

(4) Scaling circuits. The pulses from the Geiger counters were recorded by scaling circuits of British design (36). Each unit is a scale of 1,10 or 100, consisting of two cascaded scales of 10 operating on the 8+2 principle. When used as a scale of 100, a mechanical register counts once for every 100 pulses fed into the input. At the same time, an auxiliary relay closes instantaneously, so that external timing or recording apparatus can be operated. The scaling units can be connected together in cascade to form scales of 1000 or 10,000, etc.

(5) Automatic operation.

Most of the experimental curves presented in the results of this experiment were recorded automatically, and manual counting was reserved for exploratory surveys and calibration runs. The method of automatic counting used is equal to manual counting in accuracy and reliability, and has the advantage of running twenty-four hours per day. In addition the automatic system is superior in

percent utilization of counting time. A brief description of the system will be given.

The center of the system is a 50-contact, two-circuit stepping relay. One of the circuits has the moving contact connected to the output of the coincidence amplifier; all the fixed contacts of odd number (1,3,5-----49) are connected together to a scale of 10 or 100 (the waiting scaler) and all the even-numbered fixed contacts (2,4,6 ----50) to a scale of 1000 or 10,000 (the counting scaler). Thus, every single advance of the stepping relay contact switches the pulses from one scaler to the other. The second circuit of the stepping relay has the moving contact connected to the reference voltage input of the current stabilizer, and the fixed contacts are connected together in pairs (1-2, 3-4, ...49-50) to 25 closely spaced adjustable voltages, supplied by a storage cell. The stepping relay is advanced by one step every time either of the two scalers reaches its full count, and each advance of the relay is marked by a pulse on the uniformly moving tape of a graphic ammeter. A second graphic ammeter monitors the coil current continuously.

The action of the automatic system can now be explained: suppose the relay is at contact no.2, so that the counting scaler is operating. At the 10,000th pulse, the counting scaler advances the stepping relay to no.3, simultaneously shifting the counts to the waiting scaler and changing the reference voltage to the stabilizer. During the few seconds in which the stabilizer is seeking its new balance, the waiting scaler counts up to 100, and at that point advances the stepping relay to no.4, turning on the counting scaler and leaving the new current flowing in the coils. The operation then repeats. After 25 such repetitions, the whole cycle of currents and

counts is repeated. Under this scheme, the moving tape contains a record of runs of 10,000 counts at each of 25 currents in the coil, the distance between marks on the tape giving the time for 10,000 counts. The time lost in changing currents is only 1% of the total. This system has proved very reliable, and the large amount of data required could not have been collected by manual counting.

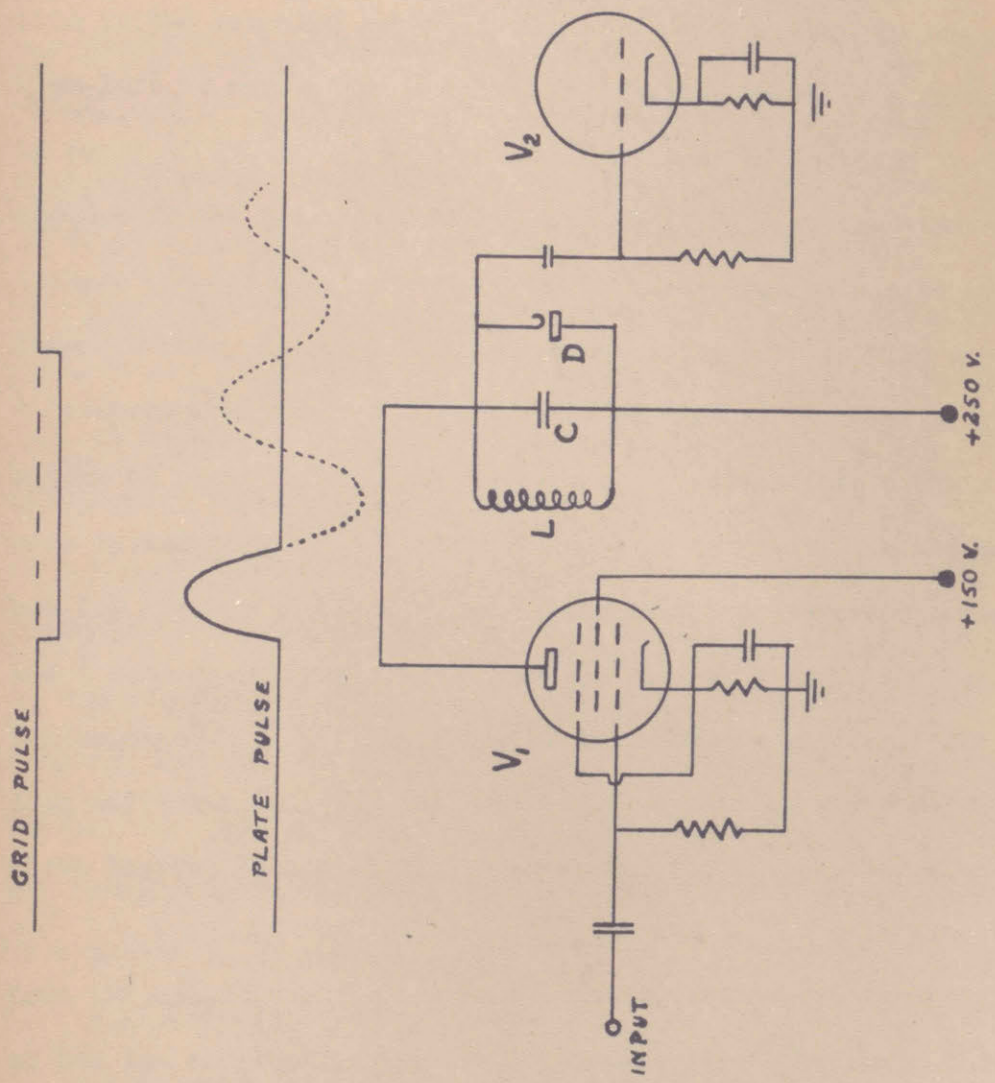

Figure 15

V. Final Experimental Arrangement.

The final arrangement of the spectrometer at the pile is illustrated in Fig.16 (see also Fig.11). The left-hand part of the drawing represents the thermal column of the Chalk River Pile. The thermal column consists of a long column of graphite blocks several feet square in cross-section, leading through the shielding wall of the pile to the reactive portion. Neutrons diffuse through the graphite from left to right, their intensity dropping by about a factor of 2 in every 30 cm. of travel. Part of the loss of neutrons is due to capture in the graphite and its impurities, and the remainder to leakage out the sides of the column. The column is closed by a Cd-lined Pb door, 25 cm. thick and faced on the outside with sheet iron. A "neutron howitzer" (A-B in Fig.16) was formed by removing graphite blocks at the outer end of the column: the dimensions of this howitzer were varied to vary the effective neutron intensity for the experiment, but for most of the final runs it was 25 inches square in cross-section and 5 feet deep. The thermal neutron flux at A under the conditions of the experiment was of the order of 10^8 neutrons/cm^2/sec. Due to the long diffusion path for the neutrons, the flux of neutrons of energy above thermal is negligible at the outer end of the thermal column.

γ-rays from the reacting portion of the pile also travel down the column towards the spectrometer, attenuated strongly according to the law $\exp(-\mu_\gamma x)$, where x is distance from the inner end of the thermal column. Of these γ-rays, only those of about 10 Mev energy

and higher (if any exist) can penetrate the graphite in a manner comparable with the neutrons. A large γ-ray intensity is being generated continuously along the length of the column by the capture of neutrons in the graphite. The intensity of this γ-radiation varies along the column roughly as exp $(-\mu_n x)$ where μ_n is the effective neutron absorption coefficient (actually due to capture plus leakage, see above).

Two source arrangements are possible at the outer end of thermal column. These are referred to as the neutron collimation method and the γ-ray collimation method. The two methods each have advantages for the study of neutron capturers with different properties.

Neutron collimation method. This method is applicable to capturers of very large cross-section, especially when they are available only in small quantities. The space A-B (Fig.16) is left empty, and the cone C is lined with a strong neutron absorber which does not produce γ-rays which would interfere with the observations. The material used here was a layer of boron in the form of B_4C, backed by a Cd sheet to be sure that any neutrons escaping capture in the boron would not escape from the door of the pile. The sample of capturer is situated at D, immediately outside the thin Cu sheet which closes the spectrometer, and is exposed to the flux of neutrons entering the solid angle defined by the cone C. The sample of capturer then acts like a small radioactive source in the spectrometer, and the discussion of Section I applies.

γ-ray collimation method. This method can be used for neutron capturers of large or small cross-section available in large quantities. On this scheme, the face A of the neutron howitzer is lined with a layer of the capturing material of sufficient thickness to absorb a large fraction of the incident neutrons without absorbing a large fraction of

the γ-rays generated: that is, a thickness of about $1/\mu_n$ or $1/\mu_\gamma$, whichever is the smaller. The entrance B of the collimating cone C is covered typically with a boron layer to prevent the escape of neutrons. The γ-rays generated in the layer at A are collimated by the cone C and fall on a circular area of diameter 6 mm. of the thin Cu sheet closing the spectrometer. This area then acts towards the spectrometer as if there were a radioactive source immediately behind it, except that the γ-rays are now fairly strongly collimated.

The γ-ray collimation method has been used only in preliminary experiments on Cd, with a 0.5 mm. sheet of Cd at A and another similar sheet at B. It is clear, however, that the γ-ray collimation method is actually in operation at all times for neutron capture in the graphite, no matter which method is being used for the sample under study. In all studies of capture γ-rays using the arrangement of Fig.16, therefore, the capture γ-rays generated by neutron capture in the graphite are always present as a background. Since C^{12} is not expected to capture neutrons appreciably, we expect the capture γ-rays from the graphite to arise chiefly from neutron capture by C^{13}. An analagous case exists for O^{16}, O^{17} and O^{18}(37).

The more exact details of the experimental arrangements will be given with the experimental results.

The presence of the iron facing of the lead door of the thermal column would be expected to alter the distribution of the magnetic field of the spectrometer. Experimentally, however, the transmission was not seriously affected. The effect on the linearity of the calibration of $H\rho$

versus coil current was checked by running over the 2.62 Mev line of ThC" - ThD in opposite directions. Any hysteresis would appear as a shift in position of the line. No such shift was detected within the limit of accuracy, about 0.1%.

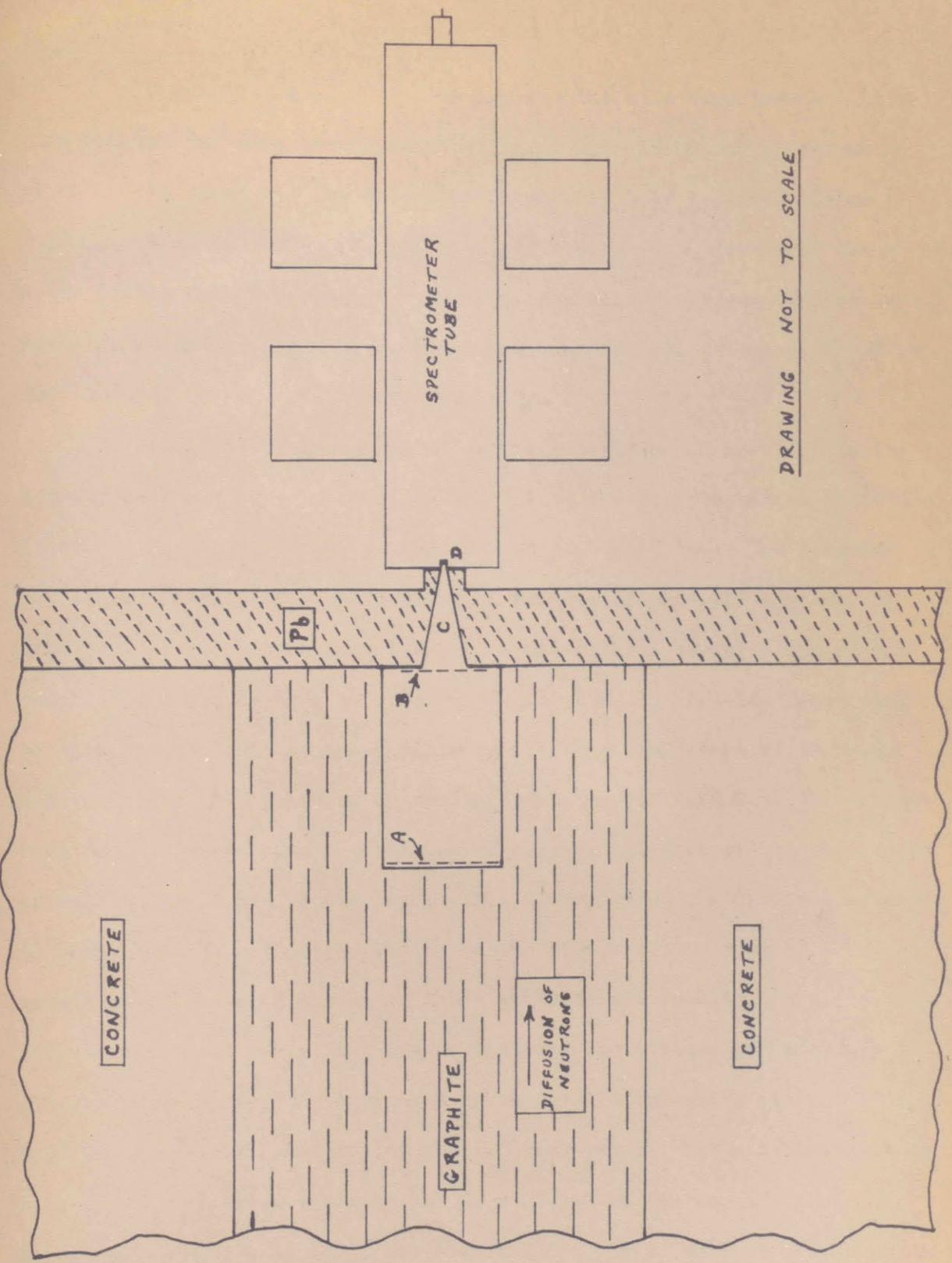
SPECTROMETER TUBE
DRAWING NOT TO SCALE
Pb
C
D
B
A
CONCRETE
GRAPHITE
DIFFUSION OF NEUTRONS
CONCRETE

Figure 16

CHAPTER 3. PRELIMINARY SPECTROMETER EXPERIMENTS

I. Search for a 3.20 Mev γ-ray from ThC"

During the period of planning for the main experiments on capture γ-rays, two experiments were performed with the β-ray spectrometer, of which the first will be described briefly in this section. Since the 2.62 Mev γ-ray of ThC"- ThD was used for the $H\rho$ calibration of the spectrometer in the main experiments, and since the same γ-ray was used in experiments on radiator thicknesses (Chapter 2, Section I), this experiment on ThC" entered the procedure very naturally.

Ellis (38) has commented on the importance of knowing the intensity of the γ-ray of energy 3.20 Mev from the disintegration ThC"-ThD, in assigning nuclear spins to the excited states of ThD. The 3.20 Mev γ-ray is predicted in the disintegration schemes of ThC"-ThD advanced by Arnoult (39) and Oppenheimer (40). The two schemes agree in their main details, and the one due to Oppenheimer is shown in Fig. 17. According to this scheme, most of the β-disintegrations of ThC" take place to an excited state of ThD having an excitation energy of 3.20 Mev. De-excitation of this state occurs mainly by successive emission of the two γ-rays of 0.58 and 2.62 Mev respectively. Ellis summarizes the previous attempts to observe the γ-ray corresponding to the direct 3.20 Mev transition and adds a measurement of his own. These attempts all resulted in claims to have observed the γ-ray, but due to the very low statistical accuracy in all the experiments, the estimates given for its intensity varied from 0.8% to 12% of the intensity of the 2.62 Mev γ-ray. The actual existence of a 3.20 Mev excited state in ThD is attested by the results of Alichanow and Dzelepow (41), who observed the positrons from internal pair production due to a transition of 3.20 Mev energy in ThC"-ThD.

A search was made for the 3.20 Mev γ-ray in the β-ray spectrometer, using the methods of Chapter 2, Section I (Figs. 6,7,8,9). An 82 mg/cm^2 uranium radiator was used in the final runs and a typical result is shown in Fig. 18. Here the height of the photoelectron line due to the 2.62 Mev γ-ray is 19,500 counts per minute. To the right the scale has been expanded by a factor of 50, and it will be seen that the low background counting rate in this region makes the search for the 3.20 Mev line very sensitive. Taking account of the variation of the photoelectric cross-section with energy, a 3.20 Mev γ-ray of intensity 0.2% of that of the 2.62 Mev γ-ray would give a line of 30 counts per minute at the position marked 3.085 Mev in Fig. 18. No such line is visible, even though the line height just quoted is more than 3 times the standard deviation of the points shown. The conclusion is that no γ-ray of energy 3.20 Mev is observed, and that such a γ-ray, if it exists, must have an intensity of less than 0.2% of the 2.62 Mev γ-ray. This result disagrees markedly with the previous measurements, and throws doubt on the spin assignments of the Oppenheimer disintegration scheme.

A more extended description and discussion of this experiment is being prepared for submission to the Canadian Journal of Research (42).

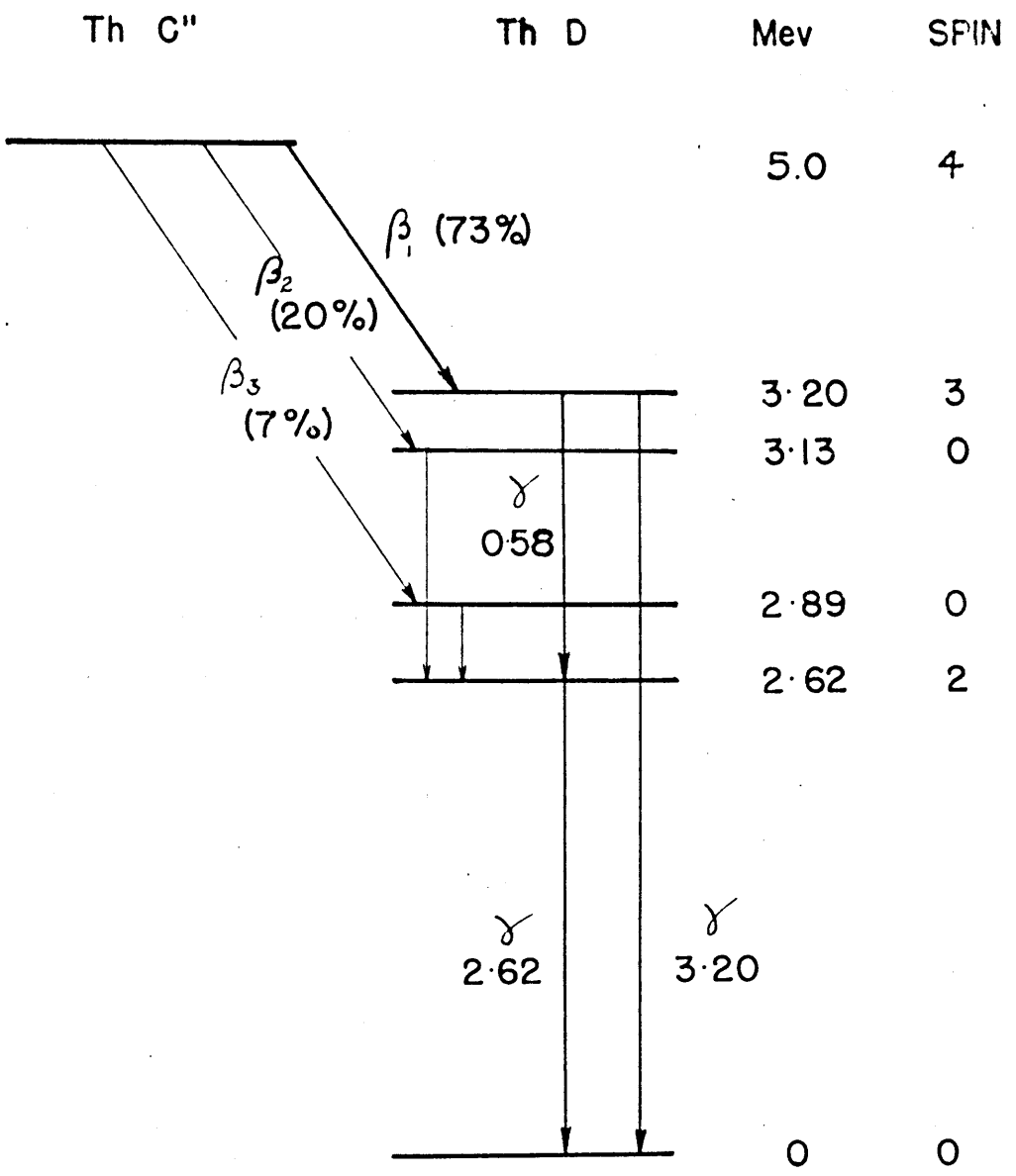
Th C"
Th D
Mev
SPIN
5.0
4
β1 (73%)
β2 (20%)
β3 (7%)
3·20
3
3·13
0
γ 0·58
2·89
0
2·62
2
γ 2·62
γ 3·20
0
0

Figure 17

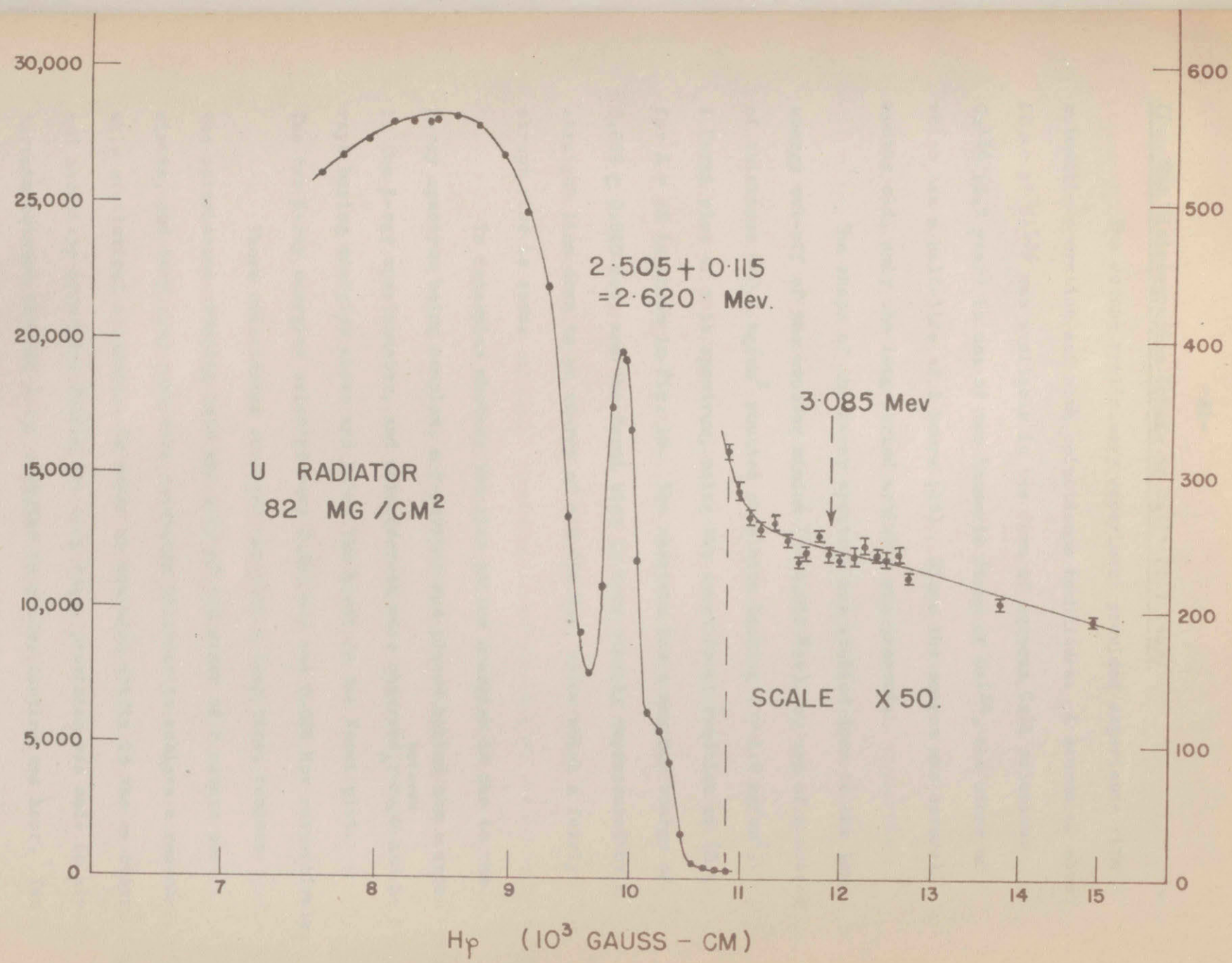
30,000
25,000
20,000
15,000
10,000
5,000
0
600
500
400
300
200
100
0
7
8
9
10
11
12
13
14
15
2·505 + 0·115
= 2·620 Mev.
3·085 Mev
U RADIATOR
82 MG/CM²
SCALE X 50.
COUNTS PER MINUTE
Hρ (10³ GAUSS - CM)

Figure 18

II. The Disintegration Scheme of Cs^{134} (1.7 Year)

The second preliminary experiment provided experience with automatic operation and with coincidence techniques. A source of about 50μc of Cs^{134} was available in the form of aqueous CsCl solution. Cs^{134} (1.7 year) is one of two isomeric forms of Cs^{134}, the other of which has a half-life of 3 hours (43). Since the source was several months old, only the long-period activity was present.

The shape of the β-ray spectrum was studied down to the low energy cut-off of the counter window ($\sim$ 0.015 Mev), by use of a source of thickness $\sim$ 0.1 mg/cm^2 mounted on a mica backing ($\sim$ 1.0 mg/cm^2). A Fermi plot of this spectrum, using the exact Fermi function of (Z,η) for Z = 55 is shown in Fig. 19. The spectrum has a maximum energy of 0.658 $\pm$ 0.030 Mev, and the Fermi plot is very closely represented by a straight line down to an energy of $\sim$ 0.090 Mev, below which a fairly abrupt rise is seen.

To determine whether the rise at low energies is due to the β-ray spectrum being complex, a γ-counter was placed behind the source in the β-ray spectrometer, and coincidences were observed between γ-rays and β-rays having energies above and below the break in the Fermi plot. The two β-ray energies selected were 0.250 Mev and 0.035 Mev respectively.

These coincidence observations took a long time, because the coincidence counting rate was only of the order of 2 counts per minute, and very long runs were necessary in order to achieve a reasonable statistical accuracy. In order to minimize drifts in the counters and associate apparatus during the long runs, provision was made to alternate between the two β-ray energies in cycles lasting one hour. Two

reference voltages were supplied to a relay connected to the current stabilizer which would cause currents to flow in the coils to focus the two β-ray energies. The switching cycle was actuated by a cam driven at 1 revolution per hour by a graphic ammeter which was also used to monitor the counting rate of the γ-ray counter. Relays, energized by a microswitch actuated by the cam, switched the pulses between duplicate scaling circuits provided for recording the β-ray counts and the coincidence counts, in synchronism with the relay which switched the current. The length of time spent at each β-ray energy was adjusted to give about the same total number of coincidences at each energy. Each one hour cycle of operation consisted of a 24 minute run at the 0.250 Mev β-ray energy, a 32 minute run at the 0.035 Mev β-ray energy, and a 4 minute background count with zero current in the coils. The system ran day and night in a very satisfactory manner.

The results of these observations showed that on the average, each β-ray at the 0.035 Mev point is accompanied by 1.20 ± 0.03 times as much γ-ray energy as each β-ray at the 0.250 Mev point. This indicated that there is a separate low energy β-ray energy spectrum superimposed on the main β-ray spectrum. An inspection of the shape of the composite spectrum observed experimentally indicates that at the 0.035 Mev point, about half the β-rays observed are due to the low - energy spectrum and about half to the high-energy spectrum. This means that each β-ray in the low-energy spectrum is accompanied by about 1.40 ± 0.06 times as much γ-ray energy as each β-ray of the high-energy spectrum. This ratio remains unchanged when a 3mm. sheet of Pb is placed in front of the γ-ray counter, reducing its counting rate to 0.64 of its previous value. The latter fact means that the γ-rays

accompanying the β-rays of the low-energy spectrum have energies of the same order as those accompanying the β-rays of the high energy spectrum; in other words, the γ-rays accompanying the low-energy spectrum are similar in energy but larger in number than those accompanying the high-energy spectrum.

The γ-rays of Cs^{134} were observed by measuring the spectrum of photoelectrons ejected by the γ-rays from a 17 mg/cm^2 Pb radiator. The resulting experimental curve is shown in Fig. 20. Three γ-rays are observed whose energies are 0.568 ± 0.015, 0.602 ± 0.015 and 0.794 ± 0.015, with relative intensities 0.26, 1.0 and 1.0 respectively, after allowing for the energy variation of the photoelectric cross-section.

These results are consistent with the disintegration scheme shown in Fig. 21. The order of emission of the 0.602 and 0.794 Mev γ-rays is unknown. The portion of this scheme associated with the 0.658 Mev β-spectrum is in agreement with the results of Siegbahn and Deutsch (44) within the combined experimental errors. The activity available for the present work was not sufficient to observe the 5% cross-over transition reported by Siegbahn and Deutsch, and this result has been adopted from their work. It should be pointed out that if the alternative level arrangement shown as a broken line in Fig. 21 is adopted, the cross-over transition may occur from the 1.964 Mev level to the 0.602 Mev level. The accuracy of the energy measurement of Siegbahn and Deutsch is not sufficient to decide between the two alternatives.

If the β-ray spectra are extrapolated to zero energy on the assumption that each spectrum is represented by a straight line on the Fermi plot, the integrated number of β-rays in the low-energy spectrum is

about 28% of all the disintegration electrons. The close agreement of this figure with the 25% figure deduced from the γ-ray intensities is consistent with the disintegration scheme of Fig. 21 and suggests that the true shapes of these β-ray spectra may continue as straight lines on the Fermi plot to zero energy.

A summary of the above results has been published as a letter to the Editor of the Physical Review (45). A fuller report containing additional work on the internal conversion and angular correlation of the Cs^{134} γ-rays is planned for submission to the Canadian Journal of Research. Siegbahn and Deutsch (46) have published a note in the Physical Review agreeing with the revision made here of their previously proposed disintegration scheme.

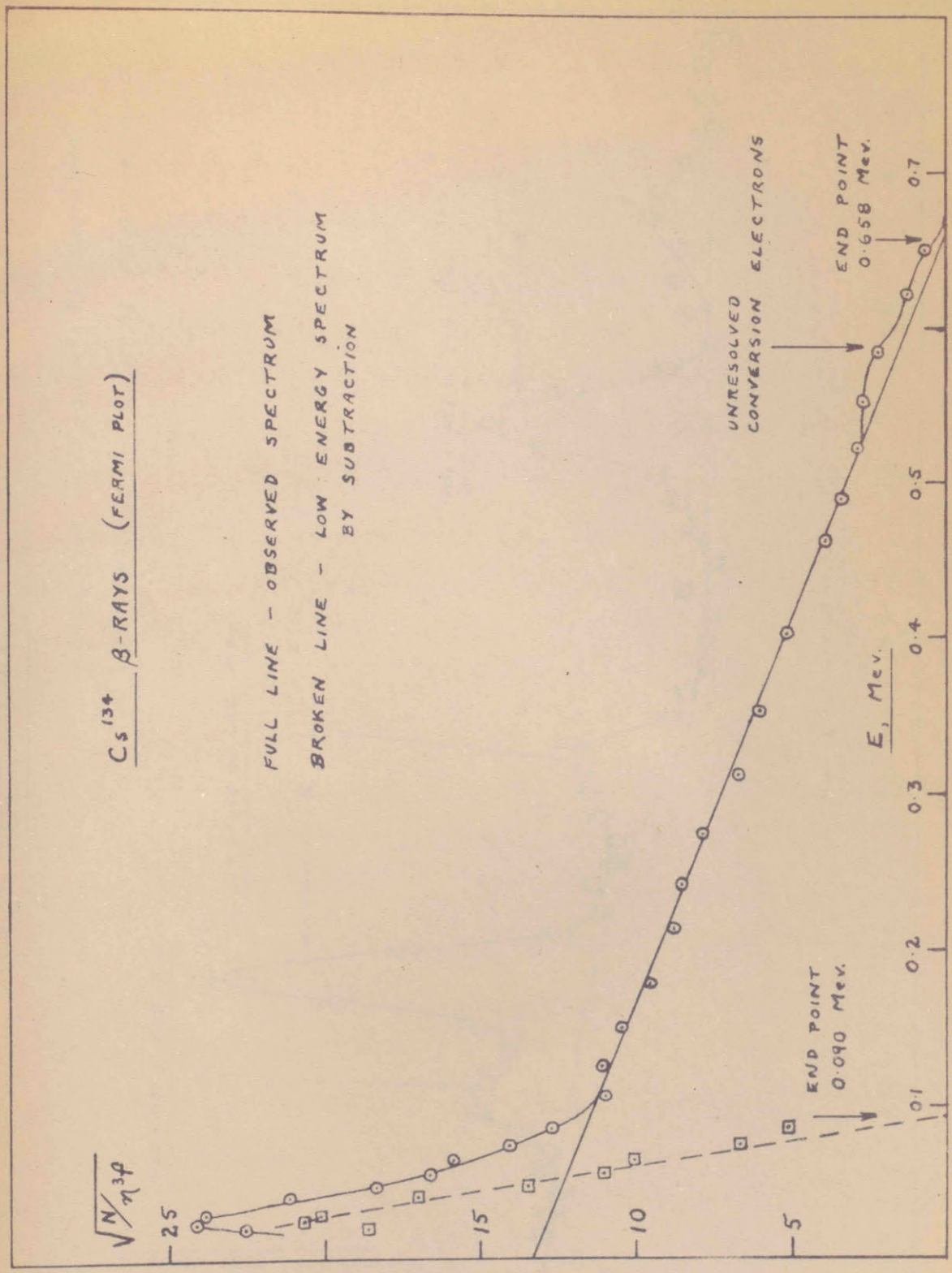
Cs^{134} β-RAYS (FERMI PLOT)
FULL LINE - OBSERVED SPECTRUM
BROKEN LINE - LOW ENERGY SPECTRUM BY SUBTRACTION
UNRESOLVED CONVERSION ELECTRONS
END POINT 0·658 Mev.
END POINT 0·090 Mev.
E, Mev.
$\sqrt{N/\eta F}$
25
15
10
5
0·1
0·2
0·3
0·4
0·5
0·7

Figure 19

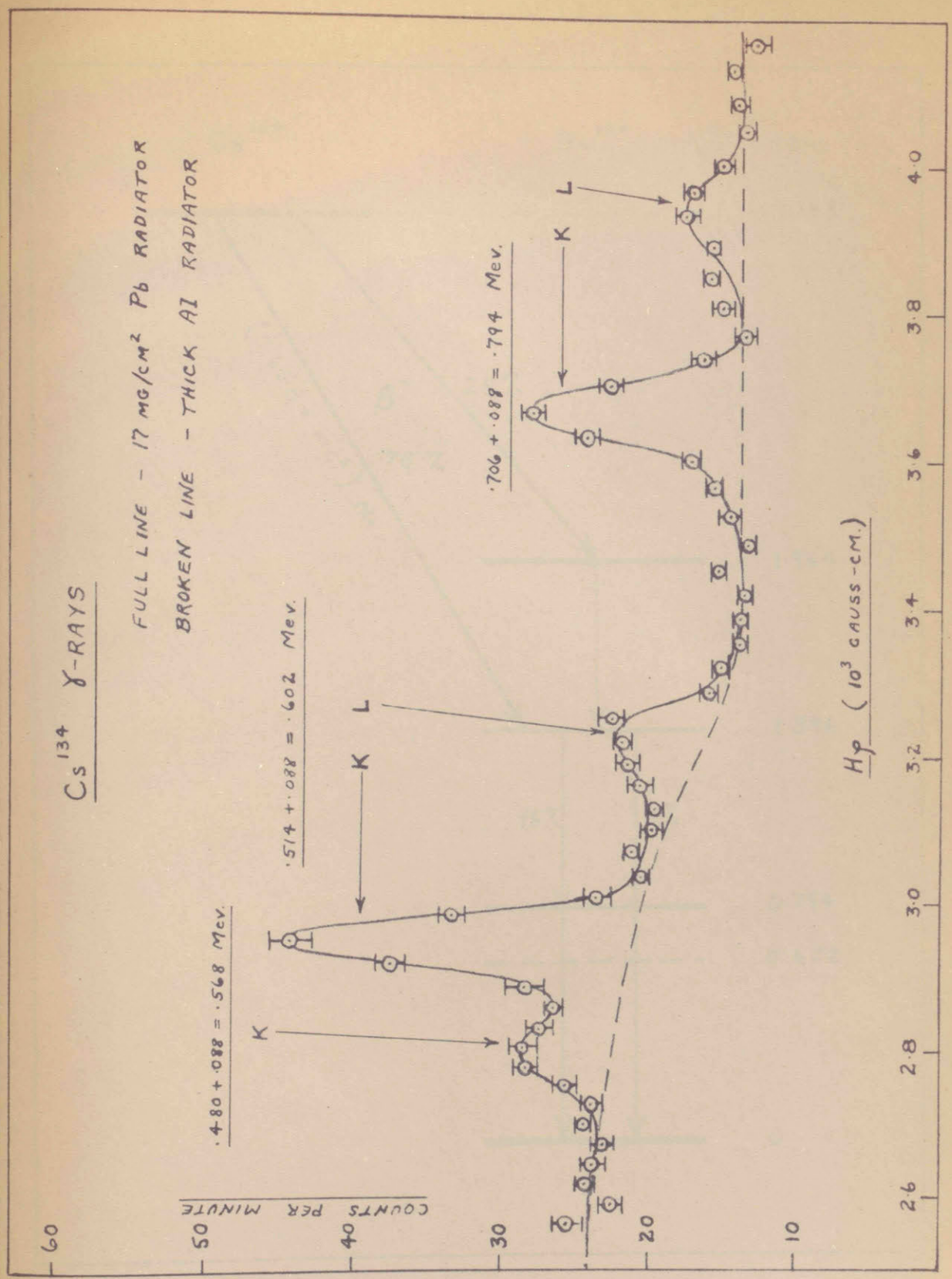
Cs 134 γ-RAYS
FULL LINE - 17 MG/CM² Pb RADIATOR
BROKEN LINE - THICK Al RADIATOR
·480 + ·088 = ·568 Mev.
·514 + ·088 = ·602 Mev.
·706 + ·088 = ·794 Mev.
K
L
COUNTS PER MINUTE
Hρ (10³ GAUSS-CM.)
60
50
40
30
20
10
2·6
2·8
3·0
3·2
3·4
3·6
3·8
4·0

Figure 20

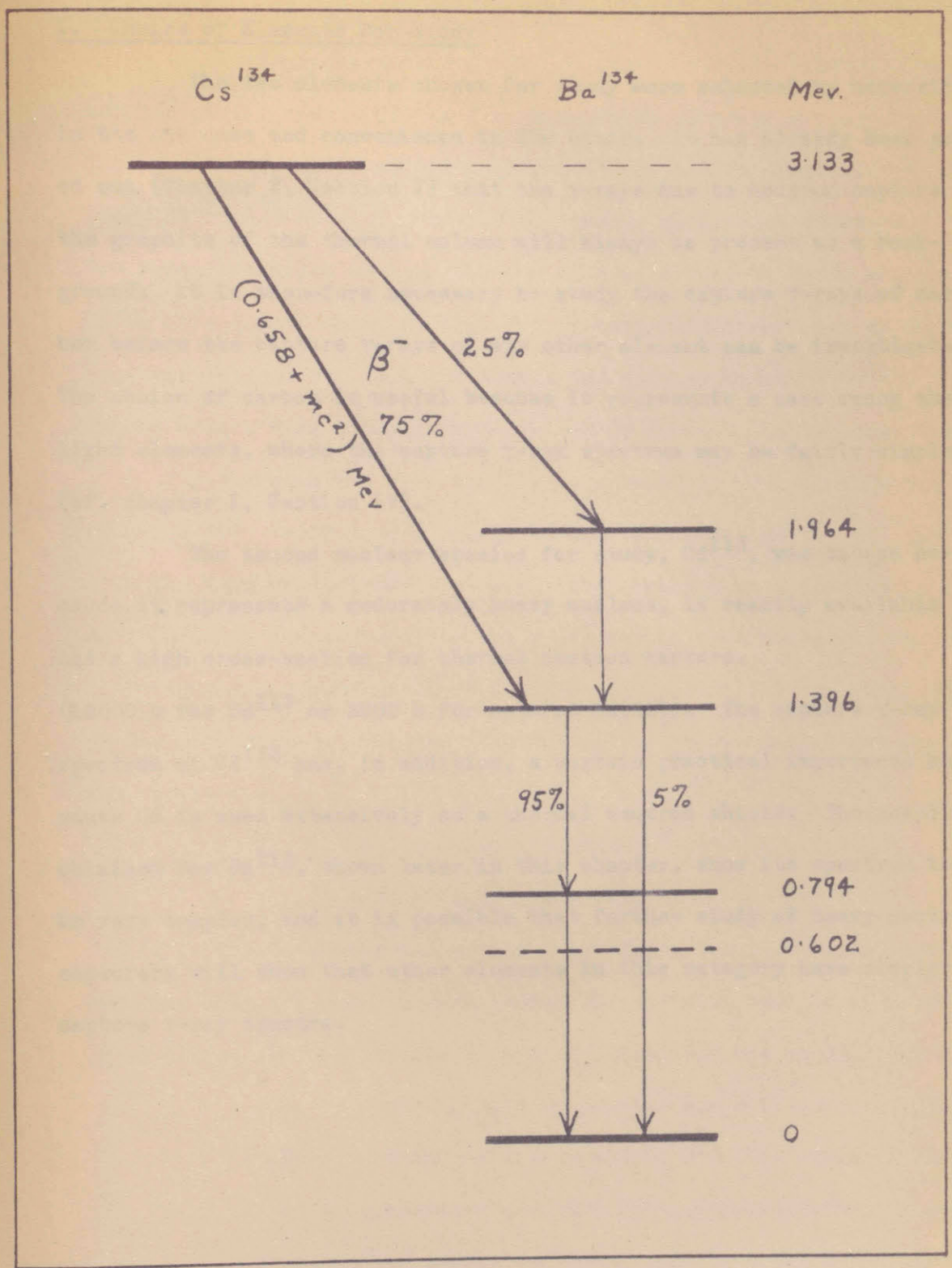
Cs 134
Ba 134
Mev.
3·133
(0·658 + mc²) Mev
β⁻
25%
75%
1·964
1·396
95%
5%
0·794
0·602
0

Figure 21

CHAPTER 4. EXPERIMENTAL RESULTS.

I. Choice of Elements for Study

The two elements chosen for study were selected by necessity in the one case and convenience in the other. It has already been pointed out (Chapter 2, Section V) that the γ-rays due to neutron capture in the graphite of the thermal column will always be present as a background. It is therefore necessary to study the capture γ-rays of carbon before the capture γ-rays of any other element can be investigated. The choice of carbon is useful because it represents a case among the light elements, where the capture γ-ray spectrum may be fairly simple (cf. chapter I, Section IV).

The second nuclear species for study, Cd^{113}, was chosen because it represents a moderately heavy nucleus, is readily available and has a high cross-section for thermal neutron capture. (20000 b for Cd^{113} or 2500 b for natural Cd(20)). The capture γ-ray spectrum of Cd^{113} has, in addition, a certain practical importance because Cd is used extensively as a thermal neutron shield. The results obtained for Cd^{113}, shown later in this chapter, show its spectrum to be very complex, and it is possible that further study of heavy neutron capturers will show that other elements in this category have simpler capture γ-ray spectra.

II. Coincidence Measurements on Cd^{113}.

Before the main experiments started, a few runs were made using a small neutron flux and a coincidence counting arrangement. The experiment was in effect a repetition of Aoki's experiment (ref. 23, and Chapter 1, Section V), using calibrated counters. Two Geiger counters of the bell-jar type were used as γ-ray counters in an arrangement shown in Fig. 22. A well-collimated beam of thermal neutrons fell on the small Cd sample and were captured by Cd^{113}. The Cd sample then acted as a γ-ray source between the two counters.

The counters were roughly calibrated by γ-γ coincidences with a Cs^{134} γ-ray source placed at the same point as the Cd sample, with the beam of neutrons shut off. The counters were assumed to have an efficiency proportional to the γ-ray energy, and using the known disintegration scheme of Cs^{134} (Chapter 3, Section II), the efficiencies of the two counters at 1 Mev were determined in the well-known way (48). The result was

$$\epsilon_A \text{ (1 Mev)} = (3.85 \pm 0.6) \times 10^{-4}$$

$$\epsilon_B \text{ (1 Mev)} = (3.65 \pm 0.6) \times 10^{-4}.$$

The Cd effect was obtained by taking the difference between two runs with the neutron beam turned on, one with and one without the Cd in place. The difference is the Cd effect and was as follows:

N_A = counting rate in counter A = 2000 counts / min.

N_B = counting rate in counter B = 1850 counts / min.

N_C = coincidence counting rate, corrected for chance coincidences and cosmic rays = 3.9 ± 0.2 counts/min.

The total energy available for γ-radiation in the capture of a

neutron by Cd^{113}, as calculated from equation (4), is 8.55 Mev. Let the total number of neutrons captured in the sample be N. Then

$$N_A = 8.55\ N \epsilon_A, \text{ or } N = \frac{N_A}{8.55 \epsilon_A}, \qquad (6)$$

Suppose that the Cd^{113} capture γ-ray spectrum consists of m γ-rays each of energy $\frac{8.55}{m}$ Mev. Here m can only denote some average number of γ-rays per neutron captured. The coincidence rate will be,

$$N_c = N \epsilon_A \epsilon_B\ (8.55)^2\ (\tfrac{m-1}{m})$$
$$= N_A \epsilon_B\ (8.55)\ (\tfrac{m-1}{m}) \text{ from (6).} \qquad (7)$$

Putting in the experimental values and solving for m,

$$m = 2.7 \pm 0.5$$

This result is chiefly of value in showing that in at least a large fraction of the cases of neutron capture in Cd^{113}, several γ-rays are emitted in succession. The capture γ-ray spectrum from Cd^{113} is thus expected to be complex to at least this extent.

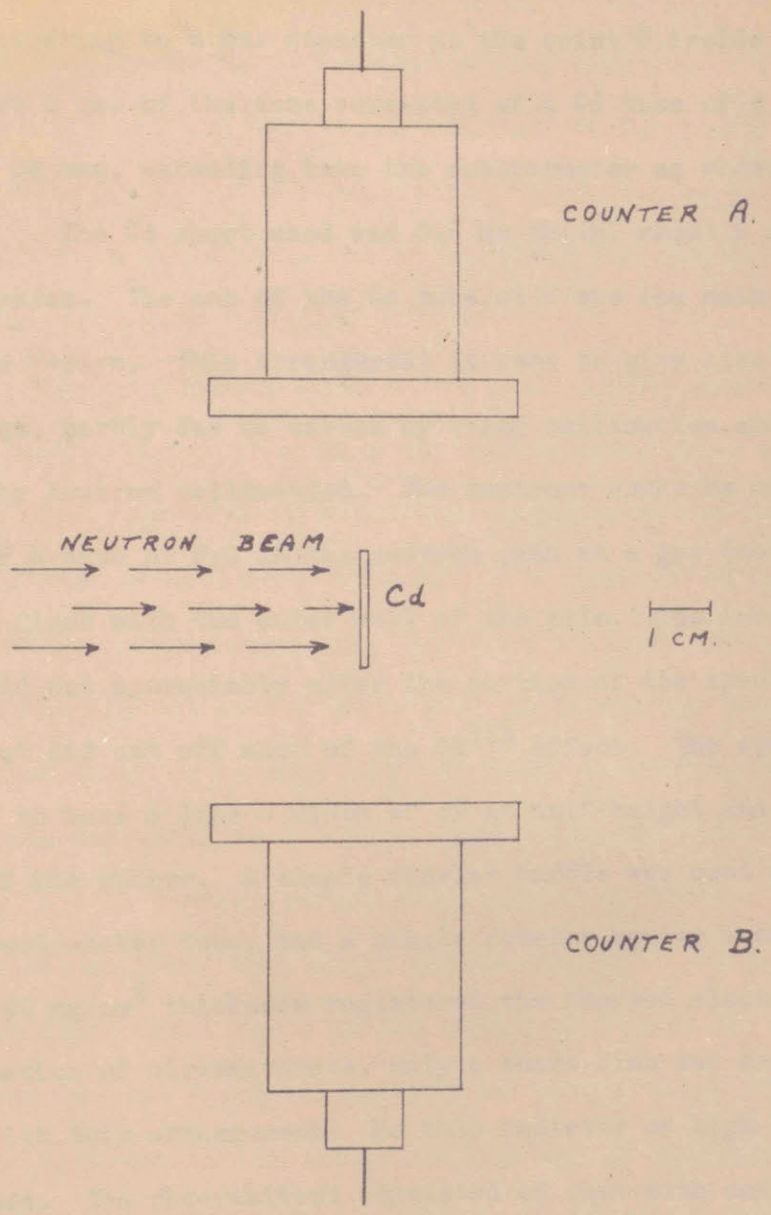

Figure 22

III. Early Spectrometer Measurements on C + Cd^{113} Spectrum

The first experimental arrangement for the observation of capture γ-rays in the spectrometer can be understood by reference to Fig. 16. The cone C was lined with Cd and had a half-angle of about 1.3°, tapering to 6 mm. diameter at the point D inside the spectrometer. The last 1 cm. of the cone consisted of a Cd tube of 6 mm. diameter with a Cd cap, extending into the spectrometer as shown at D in Fig. 16.

The Cd sheet used was 0.5 mm thick, about 9 neutron half-thicknesses. The cap of the Cd tube at D was the main source of Cd^{113} capture γ-rays. This arrangement is seen to give rise to a mixed γ-ray spectrum, partly due to carbon by γ-ray collimation and partly due to Cd^{113} by neutron collimation. The neutrons could be cut off by the insertion of a disc of B_4C in the neutron path at a gap (not shown) in the cone C flush with the outer wall of the pile. The insertion of the B_4C disc did not appreciably alter the portion of the spectrum due to carbon, but did cut off most of the Cd^{113} effect. The spectrometer was adjusted to have a line - width of 6% at half-height and a transmission of 0.5% of the sphere. A simple annular baffle was used at the center of the spectrometer tube, and a single counter having a brass window of about 20 mg/cm^2 thickness registered the focused electrons. Due to a combination of circumstances, only a short time was available for observation with this arrangement. No thin radiator of high atomic number was used. The observations consisted of runs with and without the boron disc in the neutron beam, observing chiefly the Compton recoil electrons from the Cd neutron absorber itself, with poor statistical accuracy.

The results are shown in Fig. 23. All the points shown were obtained by manual counting and the scatter of the points about the curves

drawn through them indicates the statistical accuracy obtained. The upper curve is the combined effect due to C^{13} +Cd^{113} and the lower curve should be almost entirely due to C^{13}, with possibly a small amount of Cd^{113} effect from the Cd lining of the portion of the collimating cone inside the outer face of the lead door. In any case the difference between the two curves can only be due to Cd^{113}. The low statistical accuracy of the points from which the curves were drawn does not permit a useful subtraction of the curves to obtain the effect due to Cd^{113}.

One conclusion, however, is justifiable: since the two curves of Fig. 23 are identical within the experimental error above about $H\rho$ = 24,000, the Compton recoil electron spectrum of the capture γ-rays of Cd^{113} must end at about $H\rho$ = 24,000. The maximum energy of the γ-rays from Cd^{113} is deduced from this figure as follows: the true Compton end-point of the highest energy γ-ray must lie about one full line - width (12%) below this, or at about $H\rho$ = 21,000. Converting this value to energy, the Compton end-point is 5.8 Mev. Then using the relation $E_{max.} = E_{\gamma} \cdot \frac{2E_{\gamma}}{2E_{\gamma}+mc2}$ for the Compton effect (See Chapter 2, Section I), the value E_{γ} for the capture γ-ray of highest energy from Cd^{113} is 6.03 Mev. Due to the large statistical error in the curves of Figure 23, and to the shapes of the curves, the energy of the highest energy γ-ray from Cd^{113} capture cannot be much smaller than 6.03 Mev but may be somewhat larger. The above procedure is followed in later sections in calculating γ-ray energies from experimental Compton end-points and will not be explained again.

In experiments following those just described an attempt was made to use the γ-ray collimation method for Cd^{113} as well as C^{13}, in the hope

of obtaining a greater ratio of Cd^{113} effect to C^{13} effect. A large sheet of Cd was placed at A, Fig. 16, and the entrance to the collimating cone at B was closed with a second Cd sheet. The results obtained were similar to those in Fig. 23, and a return to the neutron collimation method was made on account of the easy access to the Cd^{113} sample in the latter method. For capturers of much lower cross-section than Cd^{113}, some form of γ-ray collimation would have to be used as explained in Chapter 2, Section 5.

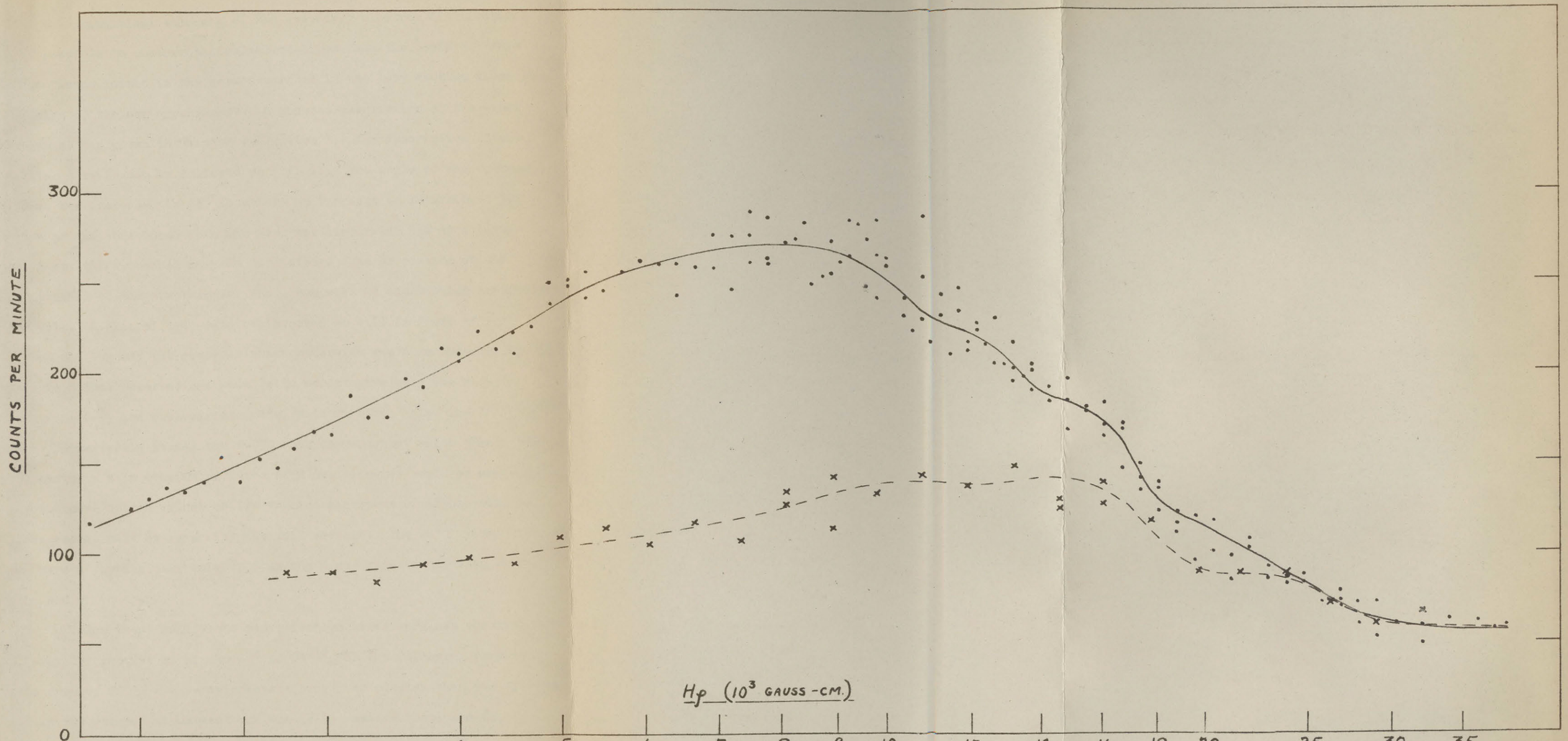
COUNTS PER MINUTE
300
200
100
0
Hρ (10³ GAUSS-CM.)
2
2·5
3
4
5
6
7
8
9
10
12
14
16
18
20
25
30
35

FIGURE 23

IV. Final Observations on C + Cd^{113}

A new experimental arrangement was made in an attempt to increase the statistical accuracy of the secondary electron distributions and if possible to observe photoelectron lines from the capture γ-rays. The experience gained in the work described in the last section aided in the design of the new arrangement. A general description of the final arrangement was given in Chapter 2, Section V. The description of the remaining details can be followed on Fig. 11. The angle of the collimating cone was increased to 15° to obtain an increase in intensity. The portion of the cone bored into the door was lined with B_4C in a layer about 2 mm. thick, backed with Cd for safety. The Bi portion of the cone attached to the spectrometer was lined with Cd sheet which constituted the sample. A disc of B_4C could be inserted at will in front of the Bi cone, cutting off the neutrons which otherwise would be obsorbed in the Cd sample. Thus observations made "with boron" give only the γ-ray effect from C^{13}, and observations made "without boron" give the C^{13} + Cd^{113} effect. Immediately inside the 0.020 inch copper sheet which closed the spectrometer a thin uranium radiator of 6 mm. diameter could be mounted. The positron-electron spiral baffle enabled electrons of either sign to be observed at will by reversing the coil current. The Cd^{113} γ-rays which were effective came chiefly from the 6 mm. diameter section of Cd at the end of the cone.

Under these conditions photoelectron lines were not observed for the γ-rays of capture of either C^{13} or Cd^{113} for the following reasons: In the case of Cd^{113} the γ-ray spectrum proved so complex that the spectrometer in its present adjustment was unable to resolve them, and the secondary electron spectrum from Cd^{113} γ-rays was a smooth curve.

In the case of C^{13} the γ-ray collimation was not effective enough to limit the effective source diameter to the nominal value of 6 mm. An estimate of the effective source diameter based on the absorbing power of Bi for γ-rays having energies of several Mev yields a value of about 20 mm. Using the method of ref. 27, this increase in source size increases the line width of the spectrometer from 3% at half-height to 7% at half-height. At this poor resolution photoelectron lines were not observed. Experiments which support this conclusion are reported later in this section.

Secondary electron distributions were observed under three sets of conditions, for both positrons and negative electrons:

Condition 1: with boron (i.e. C^{13} effect alone) with 450 mg/cm^2 U radiator.

Condition 2: without boron (i.e. C^{13} + Cd^{113} effect) with 450 mg/cm^2 U radiator.

Condition 3: with boron (i.e. C^{13} effect alone), no radiator. All the observations presented here were taken with the automatic system described previously. No point was accepted for plotting if fewer than 10,000 counts were recorded for it, and many points plotted represent over 100,000 counts. The statistical accuracy of all points therefore is 1% or better. For conditions 1 and 2 at high energies ($H\rho$ = 22,000) a sheet of aluminum of thickness 800 mg/cm^2 was placed in front of the window of counter C_2 (Fig.11). This step reduced the background by a factor of 3 while reducing the effect by only a factor of 1.5.

The complete set of experimental data taken in these runs is represented in Fig. 24 (negative electrons) and Fig. 25 (positrons). A

logarithmic scale of $H\rho$ has been used throughout. Each complete curve was made in four or five runs of the automatic apparatus, a typical run covering a range of about 1.5:1 in $H\rho$. The spacing between successive points is about 2 or 3% in $H\rho$ except where runs were repeated or successive runs overlapped. Most of the points shown are averages of several registrations of 10,000 counts, but some points represent a single run of 10,000 counts. The reproducibility of all curves was excellent for all runs.

Fig. 26 gives the secondary electron distribution for C^{13} with background subtracted taken from the Condition 3 curve of Fig. 24, and Fig. 27 gives the secondary electron distribution for Cd^{113} by subtraction of Condition 1 from Condition 2 in Fig. 24.

The C^{13} distribution is seen to consist mainly of three distinct superimposed recoil electron distributions each similar in shape to that of Fig. 10. The outlines of the three distributions have been extended with broken lines. The end-points are at $H\rho$ = 13,800, 18,500 and 28,000 respectively, corresponding to γ-ray energies of 3.50 ± 0.10, 4.65 ± 0.15 and 7.15 ± 0.25 Mev respectively. The relative intensities may be estimated from the areas under the curves (taking into account the increasing scattering losses in the coincidence counters as we go to lower energies) as 1.0 ± 0.5, 1.0 ± 0.3 and 1.0 respectively. The secondary electron distribution at the highest energy has a slight tail to the high-energy side whose origin is unknown.

The secondary electron distribution due to Cd^{113} in Fig. 27 is remarkable in presenting no features for analysis other than its extreme smoothness and fairly definite end-point. The smoothness can only mean

that the Cd^{113} γ-ray spectrum is sufficiently complicated so that the separate γ-rays cannot be resolved. Judging by the appearance of the distribution due to C^{13}, where three γ-rays appear with an average spacing of about 2 Mev in energy, we can say that the average spacing between the Cd^{113} γ-rays must not be greater than, say, 1 Mev and is possibly very much smaller. The end point of the recoil electron distribution occurs at $H\rho = 25,300 \pm 2\%$ yielding an energy of 6.20 ± 0.15 Mev for the γ-ray of highest energy detected in the Cd^{113} spectrum. This energy agrees satisfactorily with the one obtained from Fig.23.

The positron distributions of Fig.25 serve mainly to support the conclusions of the analysis of the secondary electron spectrum and the argument about effective source diameters. Since the pair-production cross-section increases as Z^2, the pair production from a given thickness of radiator in mg/cm^2 increases about as Z. Thus the copper sheet closing the spectrometer at the source end is about $\frac{29}{29} = 0.3$ as effective as a thick sheet of U in producing positron-electron pairs. The two curves Condition I and Condition 3 in Fig. 25 show that the ratio of the yield of positrons with and without the U radiator of 6 mm. diameter is much smaller than expected on the above analysis. This means that the effective source diameter is much larger than 6 mm. and agrees with the argument to the same effect earlier in this section.

Only two clear uprises are seen on the Condition 1 positron curve, the end-points being $H\rho = 25,000 \pm 5\%$ and $H\rho = 15,500 \pm 5\%$, corresponding to γ-ray energies of 7.0 ± 0.35 and 4.6 ± 0.25 Mev respectively. The positron rise due to the γ-ray of 3.5 Mev should have its end-point at $H\rho = 11,4000$. At this point on the curve there is only a slight indication of the positron rise due to this γ-ray. The reasons

for this small effect are the drop in counter efficiency and the decrease of the pair production cross-section with decreasing energy. The two γ-ray energies deduced from the positron spectrum are in satisfactory agreement with those deduced from the secondary electron spectrum.

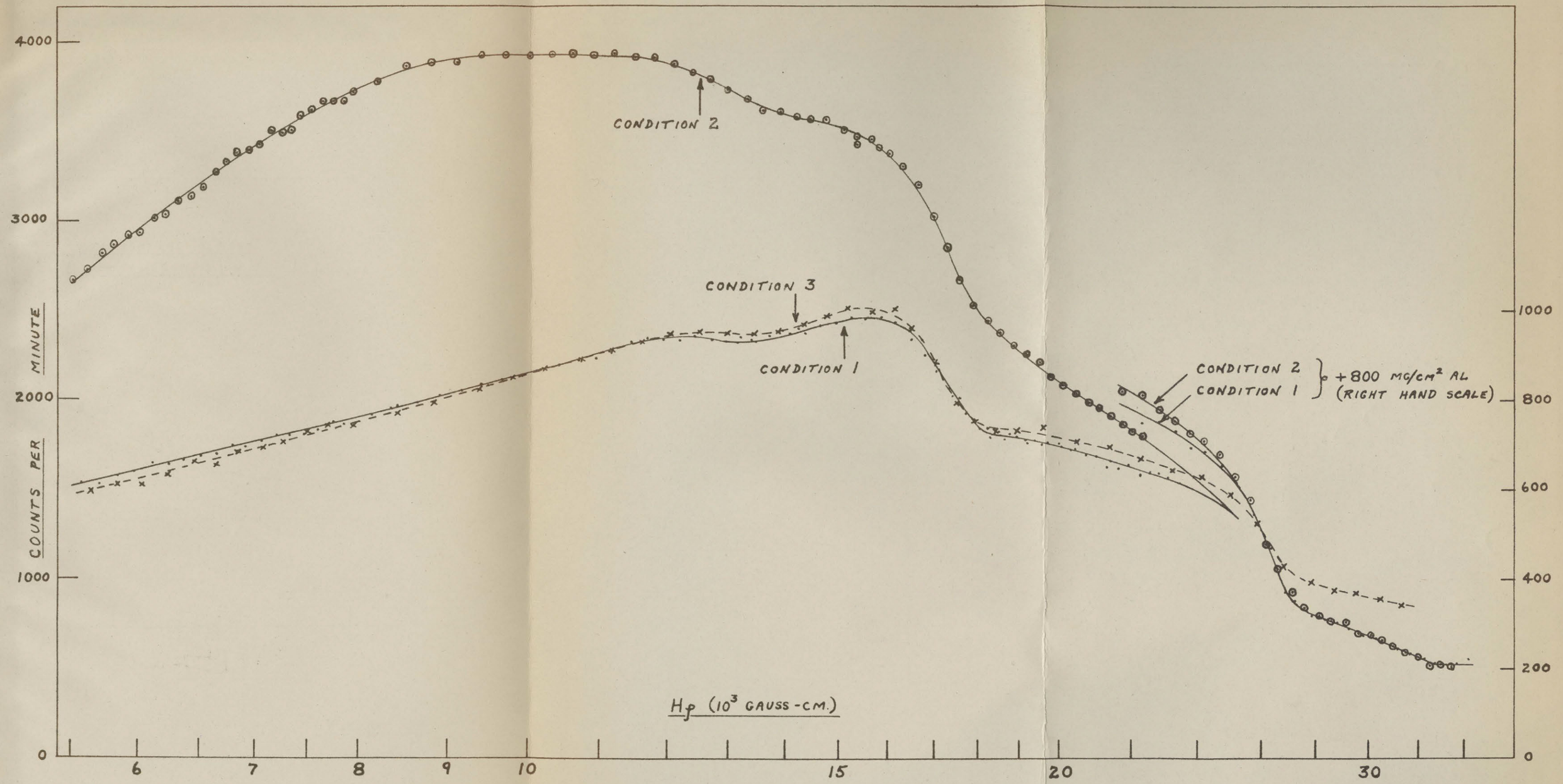
4000
3000
2000
1000
0
COUNTS PER MINUTE
CONDITION 2
CONDITION 3
CONDITION 1
CONDITION 2
CONDITION 1
+800 MG/CM² AL
(RIGHT HAND SCALE)
1000
800
600
400
200
0
Hρ (10³ GAUSS-CM.)
6
7
8
9
10
15
20
30

FIGURE 24

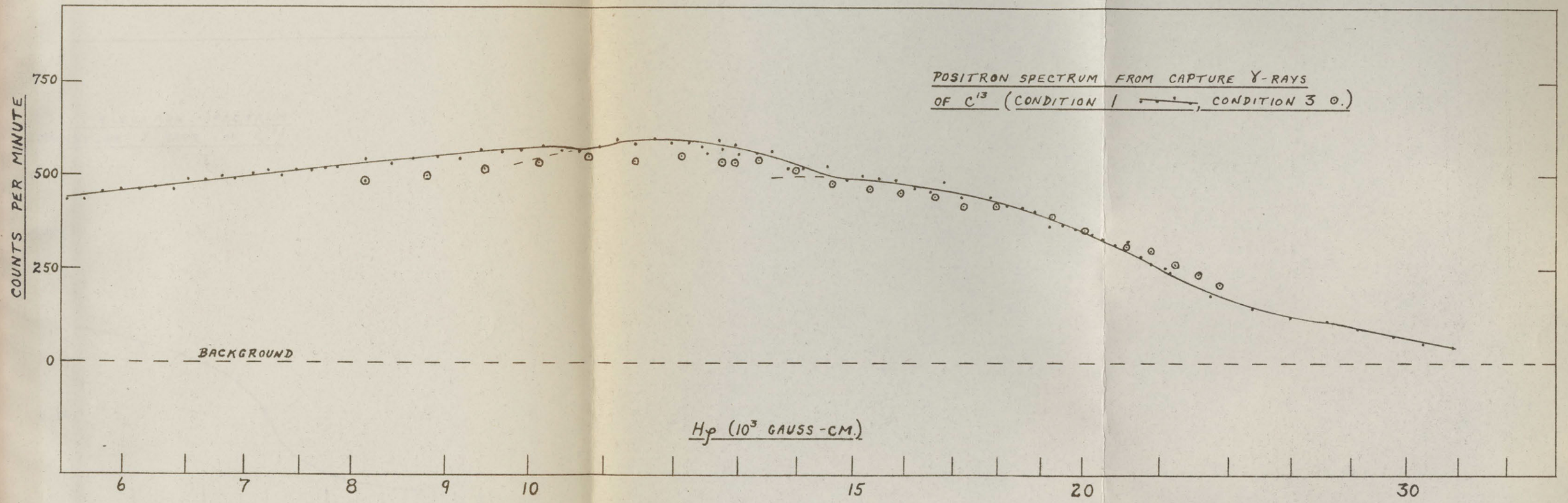
POSITRON SPECTRUM FROM CAPTURE γ-RAYS
OF C13 (CONDITION I ——, CONDITION 3 o.)
COUNTS PER MINUTE
750
500
250
0
BACKGROUND
Hρ (10³ GAUSS-CM.)
6
7
8
9
10
15
20
30

FIGURE 25

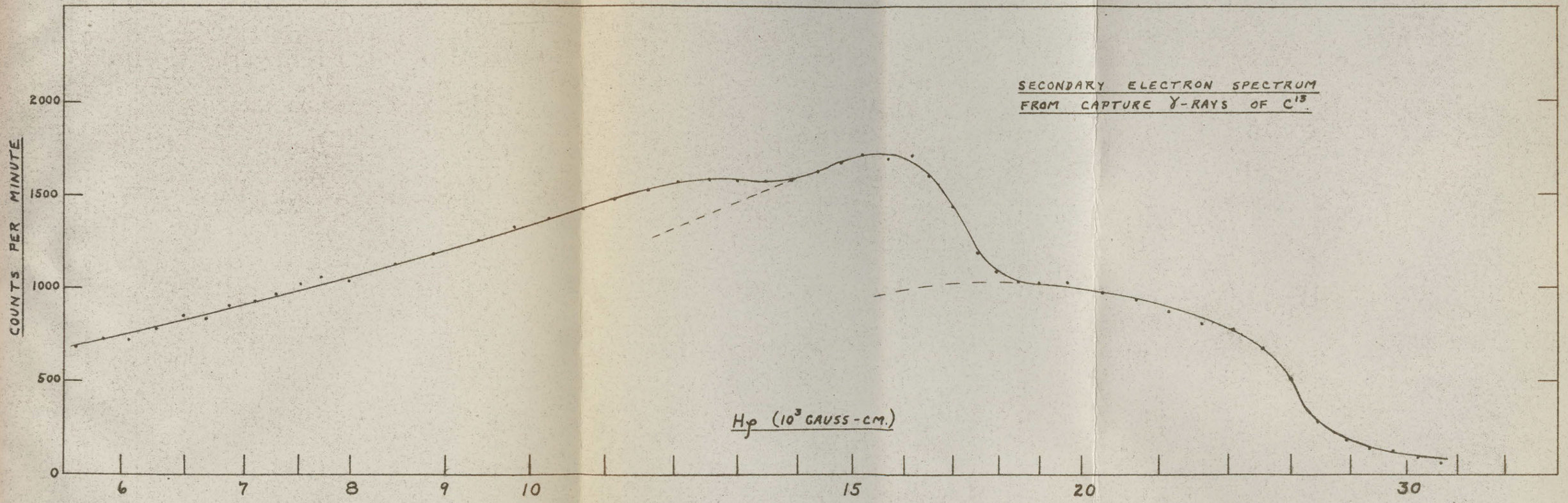
SECONDARY ELECTRON SPECTRUM
FROM CAPTURE γ-RAYS OF C13
COUNTS PER MINUTE
2000
1500
1000
500
0
Hρ (10³ GAUSS-CM.)
6
7
8
9
10
15
20
30

FIGURE 26

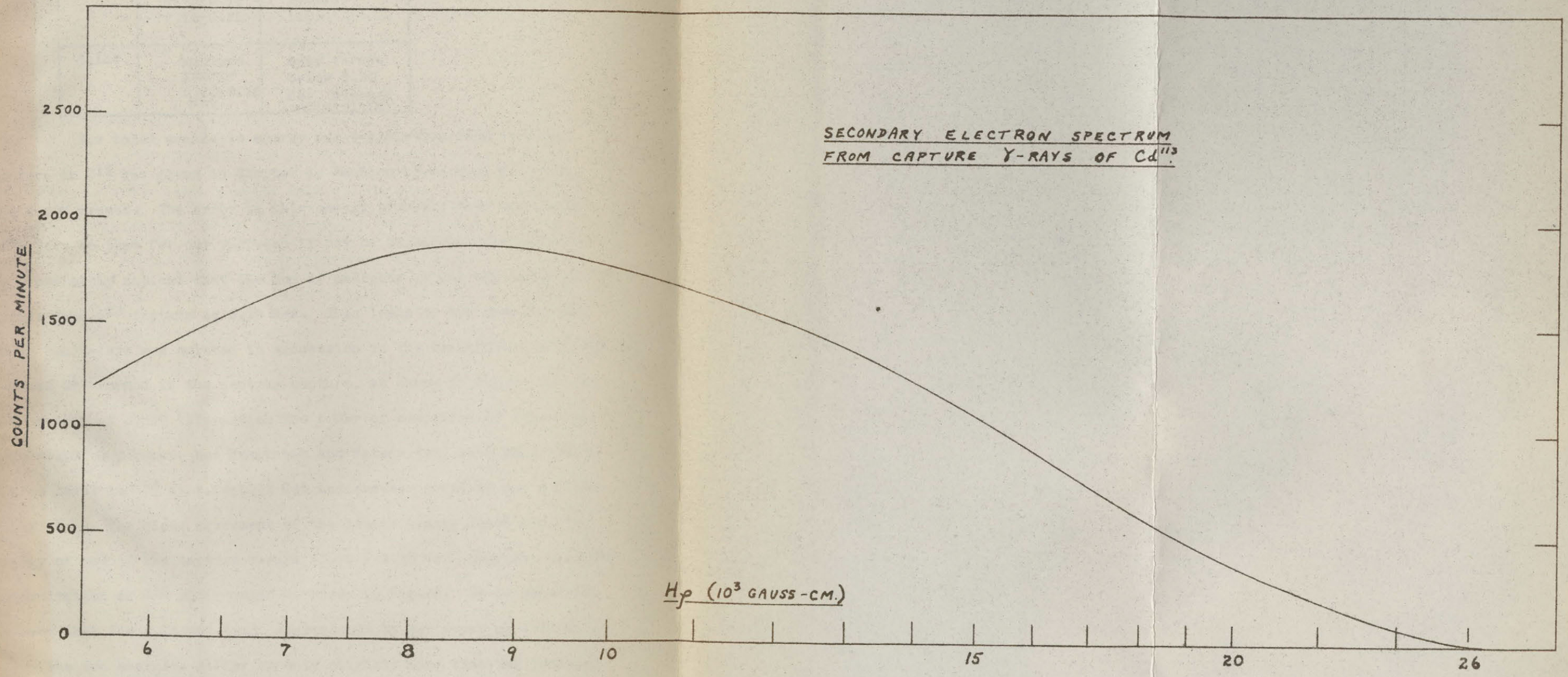
SECONDARY ELECTRON SPECTRUM
FROM CAPTURE γ-RAYS OF Cd113
COUNTS PER MINUTE
2500
2000
1500
1000
500
0
Hρ (10³ GAUSS-CM.)
6
7
8
9
10
15
20
26

FIGURE 27

V. Summary and Discussion of Results

The results obtained for the γ-rays due to neutron capture in C^{13} and Cd^{113} are summarized as follows:

C^{13}	Energy of γ-rays	Relative intensity of γ-rays.
	3.50±0.10 4.65±0.15 7.15±0.25	1.0±.5 1.0±.3 1.0
Cd^{113}	maximum energy 6.20±0.15 Mev.	many γ-rays below 6.20 Mev, average spacing<1 Mev

The total available energy for γ-radiation from neutron capture in C^{13} was given in Chapter 1, Section IV as 8.16 Mev from the known masses. The error in this energy probably does not exceed 0.06 Mev, so that for our purposes it may be considered certain. It is immediately noticed that the sum of energies of the two lower-energy γ-rays from C^{13} capture is 8.15 Mev. This leads to the surmise that these two γ-rays are emitted in succession in the de-excitation of the excited C^{14} formed in the neutron capture, as shown in Fig.3 (b). In the absence of other information the order of emmission of these two γ-rays would be unknown, but Humphreys and Watson (48) have measured an energy level in C^{14} at 5.24±0.29 Mev and another possible one at 3.44 ± 0.27 Mev. The close agreement of the latter energy level with the energy of one of the capture γ-rays (3.50 ± 0.10 Mev) suggests that the de-excitation of C^{14} may proceed as shown in Fig.28. It is possible however that the 5.24 Mev level corresponds to our γ-ray of 4.65 Mev, since the two energies differ by only slightly more than the combined probable errors. The capture γ-ray of 7.15 Mev should be accompanied

by a total γ-ray energy of about 1.0 Mev, probably in the form of a single γ-ray. Since Bennett et al. (49) have found no energy levels of C^{14} below 2.8 Mev, the 1 Mev γ-ray is probably emitted first, if it exists. The cutoff of the counters in the present experiment did not permit a search in the 1 Mev region. A possible capture and de-excitation scheme for C^{13} (n,γ) C^{14} is shown in Fig. 28.

For the Cd^{113} case, fewer conclusions can be drawn. If the calculated figure of 8.55 Mev for the total energy is correct, the ending of the spectrum at 6.2 Mev means that direct transitions to the ground state do not occur in an appreciable fraction of the cases. Since the spin of Cd^{113} is 1/2 (20) and that of C^{114} should be zero (even-even nucleus), this fact probably means that the capture of a thermal neutron by Cd^{113} results in most cases in an excited Cd^{114} having spin = 0, so that the direct transition to the ground state cannot occur.

The method of observation of capture γ-rays described above, though powerful compared with previous experiments in the field, is capable of much improvement. Experimental steps can be taken to prevent the effective source diameter from becoming large as described in Section IV. These steps include the substitution of an annular cone for the collimating cone C, Figure 16, and the use of auxiliary baffles in the spectrometer to limit the effective source size. Photoelectron lines would then be observed in spectra such as that of C^{13} and more detail might appear in spectra such as that of Cd^{113}. The method can be applied to a large number of nuclear species throughout the periodic table.

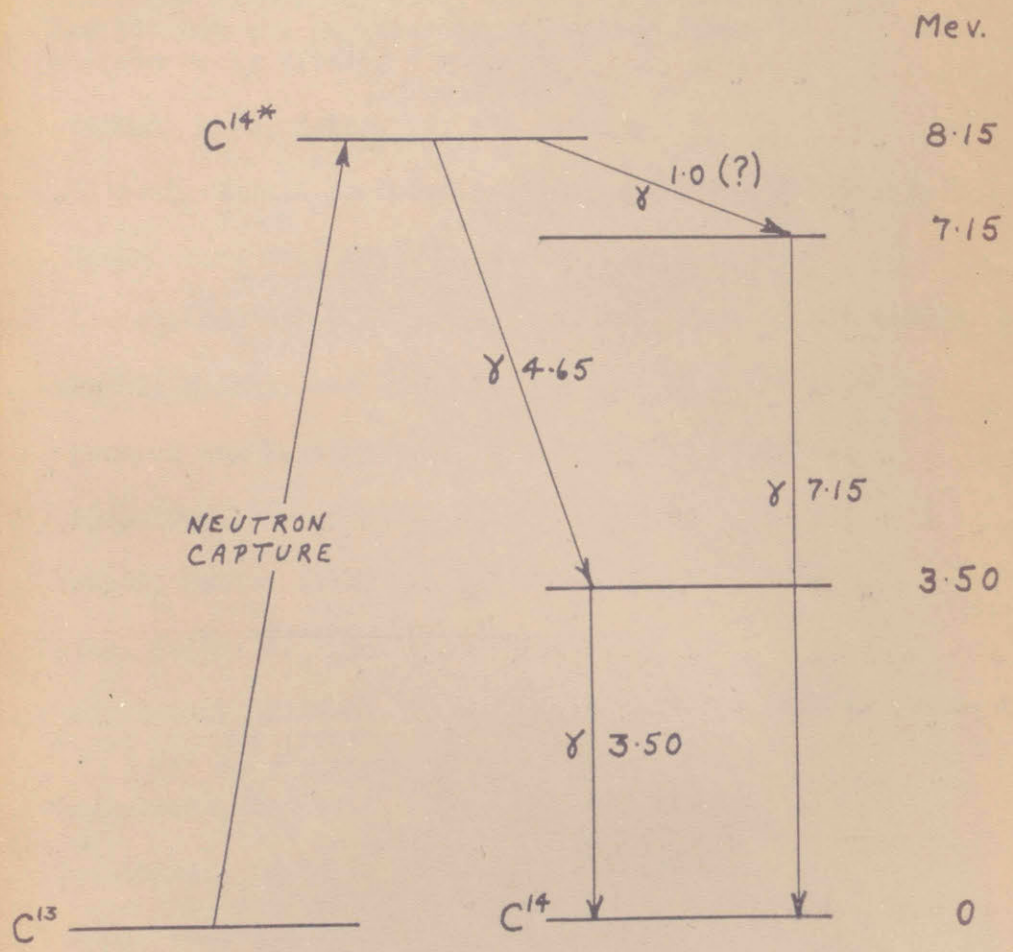
Mev.
C^{14*}
8·15
1·0 (?)
γ
7·15
γ 4·65
γ 7·15
NEUTRON CAPTURE
3·50
γ 3·50
C^{13}
C^{14}
0

Figure 28

BIBLIOGRAPHY

(1) E.Amaldi, O.d'Agostino, E.Fermi, B. Pontecorvo, F.Rasetti and E. Segrè, Proc. Roy. Soc. A149, 522 (1935).

(2) C.F. von Weizsäcker, Zeits, f, Phys. 96, 431 (1935).

(3) H.A. Bethe and R.F. Bacher, Rev. Mod. Phys. 8, 82 (1936).

(4) E. Fermi, Los Alamos lectures, quoted by M. Deutsch, "The Science and Engineering of Nuclear Power ", Addison-Wesly (1947).

(5) J. Mattauch, Phys. Zeits. 42, 116 (1941).

(6) L.G. Elliott, McGill Lectures on Nuclear Physics (1945-46).

(7) H.A. Bethe, Rev. Mod. Phys. 9, 69(1937).

(8) M.S. Livingstone and H.A. Bethe, Rev. Mod. Phys 9, 245 (1937), p.340.

(9) K. Kikuchi, H.Aoki, and K. Husimi, Nature 137, 745 (1936).

(10) J. Rainwater and W.W. Havens, Phys.Rev. 70, 136 (1946).

(11) D.E. Lea, Proc. Roy. Soc. 150A, 637 (1935).

(12) F. Rasetti, Zeits, f. Phys. 97, 64 (1935).

(13) W. Bothe, Zeits. f. Phys. 63, 381 (1930).

(14) R. Fleischmann, Zeits. f. Phys. 97, 242 and 265 (1935), Zeits. f. Techn. Phys. 16, 412 (1935).

(15) R. Fleischmann, Zeits. f. Phys. 100, 307 (1936).

(16) R. Fleischmann, Zeits f. Phys. 103, 113 (1936).

(17) C. Haenny, Comptes Rendus 203, 173 (1936).

(18) K. Kikuchi, H. Aoki and K. Husimi, Nature 137, 30, 186, 398, 745 and 992 (1936): Zeits. f. Phys. 105, 369 (1935); 18, 35, 115, 188 and 297 (1936): Proc. Imp. Acad. Jap. 11, 253 (1935). 265 (1937): Proc. Phys. Math. Soc. Jap. 17,

(19) T.W. Bonner and W.M. Brubaker, Phys. Rec. 49, 19 (1936).

(20) Segrè chart in "The Science and Engineering of Nuclear Power", Addison-Wesley (1947).

(21) B. Pontecorvo, Jour. de Phys. et le Rad. 7, 511 (1936).

(22) E.H.S. Burhop, R.D. Hill and A.A. Townsend, Proc.Roy. Soc. 165A, 116 (1938).

(23) H. Aoki, Proc. Phys. Math. Soc. Jap. 19, 799 (1937).

(24) C.D. Ellis and G.H. Aston, Roc. Roy.Soc. 129A, 180 (1930).

(25) D.V.Skobeltzyn, Zeits. f. Phys. 43, 354 (1927): 58, 595 (1929).

(26) G.D. Latyschev, Rev. Mod. Phys. 19, 132 (1947).

(27) M. Deutsch, L.G. Elliott and R.D. Evans, Rev.Sci. Inst. 15, 178 (1940)

(28) L.G.Elliott, Ph.D. Thesis, Massachusetts Inst. Tech. (1943). See also Phys. Rev. 60, 470L and 544(1941): 61, 686 (1942): 62, 3(1942): 64, 268 and 321 (1943): 65, 211 (1944): 68, 211 (1944): 68, 193 (1945).

(29) Z. Davidson and G.D. Latyschev, Jour. Phys. U.S.S.R. 6, 15 (1942).

(30) R.Sauter, Ann. der Phys. 11, 454 (1931).

(31) J.C. Jaeger and H.R. Hulme, Proc. Roy. Soc. 153A, 443 (1936).

(32) Brown Instrument Division, Minneapolis-Honeywell Company, Leaside, Ont.

(33) H. Bode, "Network Analysis and Feedback Amplifier Design," Van Nostrand (1945).

(34) L.A. McColl, "Servomechanisms," Van Nostrand (1945).

(35) H. Nyquist, Bell System Tech. Jour. 11, 126 (1932).

(36) Telecommunications Research Establishment Type 200.

(37) L. Seren, H.N. Friedlander and S.H. Turkel, Phys. Rev. 71, 463 (A) (1947). A.N. May and E.P. Hincks, Can. Jour. Res. 25, 77 (1947).

(38) C.D. Ellis, Proc. Phys.Soc. 50, 213 (1938).

(39) R. Arnoult, Ann. de Phys. 12, 241 (1939).

(40) F. Oppenheimer, Proc. Camb. Phil. Soc. 32, 328 (1936).

(41) A. Alichanow and B. Dzelepow, Comptes Rendus Acad. Sci. U.R.S.S. 20, 113 (1938).

(42) R.E. Bell and L.G. Elliott, "Search for a 3.20 Mev γ-ray in the Disintegration of Thorium C"," in preparation.

(43) G.T. Seaborg, Rev. Mod. Phys. 16, 1 (1944).

(44) K. Siegbahn and M. Deutsch, Phys.Rev. 71, 483 (A) (1947).

(45) L. G. Elliott and R.E. Bell, Phys. Rev. 72, 979 (1947).

(46) K.Siegbahn and M.Deutsch, Phys. Rev. 73, 440 (1948).

(47) F.A. Jenkins, Phys. Rev. 73, 639 (1948).

(48) R.F. Humphreys and W.W. Watson, Phys. Rev. 60, 542 (1941).

(49) W.E. Bennett, T.W. Bonner, E. Hudspeth, H.T.Richards and B.E. Watt, Phys. Rev. 59, 781 (1941).